Dnmt3a and Dnmt3b Associate with Enhancers to Regulate Human Epidermal Stem Cell Homeostasis

Cell Stem Cell

Dnmt3a and Dnmt3b associate with enhancers to regulate human epidermal stem cell homeostasis

--Manuscript Draft--

Manuscript Number:	CELL-STEM-CELL-D-15-00665R2
Full Title:	Dnmt3a and Dnmt3b associate with enhancers to regulate human epidermal stem cell homeostasis
Article Type:	Short Article
Keywords:	epidermal stem cells, enhancers, de novo DNA methyltransferases, DNA hydroxymethylation, stem cell homeostasis
Corresponding Author:	Salvador Aznar Benitah Institute for Research in Biomedicine (IRB Barcelona) Barcelona, SPAIN
First Author:	Salvador Aznar Benitah
Order of Authors:	Salvador Aznar Benitah
	Lorenzo Rinaldi
	Debayan Datta
	Judit Serrat
	Lluis Morey
	Guiomar Solanas
	Alexandra Avgustinova
	Enrique Blanco
	Jose Ignacio Pons
	David Gomez
	Alex Von Kriegsheim
	Luciano Di Croce
Abstract:	The genome-wide localization and function of endogenous Dnmt3a and Dnmt3b in adult stem cells are unknown. Here, we show that in human epidermal stem cells the two proteins bind in a histone H3K36me3-dependent manner to the most active enhancers and are required to produce their associated enhancer RNAs. Both proteins prefer super-enhancers associated to genes that either define the ectodermal lineage or establish the stem cell and differentiated states. However, Dnmt3a and Dnmt3b differ in their mechanisms of enhancer regulation: Dnmt3a associates with p63 to maintain high levels of DNA hydroxymethylation at the center of enhancers in a Tet2-dependent manner, whereas Dnmt3b promotes DNA methylation along the body of the enhancer. Depletion of either protein inactivates their target enhancers, and profoundly affects epidermal stem cell function. Altogether, we reveal novel functions for Dnmt3a and Dnmt3b through at enhancers that could contribute to their roles in disease and tumorigenesis.

Dnmt3a and Dnmt3b Associate with Enhancers to Regulate Human Epidermal Stem Cell Homeostasis

Lorenzo Rinaldi,[1,3,5] Debayan Datta,[1] Judit Serrat,[1] Lluis Morey,[6] Guiomar Solanas,[1] Alexandra Avgustinova,[1] Enrique Blanco,[3] José Ignacio Pons,[1] David Gomez Matallanas,[4] Alex Von Kriegsheim,[4] Luciano Di Croce,[2,3,5]* and Salvador Aznar Benitah[1,2]*.

[1]Institute for Research in Biomedicine (IRB Barcelona), The Barcelona Institute of Science and Technology, Baldiri Reixac 10, 08028, Barcelona, Spain. [2]ICREA, Passeig de Lluís Companys 23, 08010, Barcelona, Spain. [3]Centre for Genomic Regulation (CRG), Dr. Aiguader 88, 08003, Barcelona, Spain. [4]Systems Biology Ireland; University College Dublin; Belfield, Dublin 4, Ireland. [5]Universitat Pompeu Fabra (UPF), Dr. Aiguader 88, 08003, Barcelona, Spain. [6]Sylvester Comprehensive Cancer Centre, University of Miami, Miller School of Medicine, USA.

Co-corresponding authors Luciano.DiCroce@crg.eu;

salvador.aznar-benitah@irbbarcelona.org

Short Title: Dnmt3a and Dnmt3b regulate enhancers

Summary

The genome-wide localization and function of endogenous Dnmt3a and Dnmt3b in adult stem cells are unknown. Here, we show that in human epidermal stem cells the two proteins bind in a histone H3K36me3–dependent manner to the most active enhancers and are required to produce their associated enhancer RNAs. Both proteins prefer super-enhancers associated to genes that either define the ectodermal lineage or establish the stem cell and differentiated states. However, Dnmt3a and Dnmt3b differ in their mechanisms of enhancer regulation: Dnmt3a associates with p63 to maintain high levels of DNA hydroxymethylation at the center of enhancers in a Tet2-dependent manner, whereas Dnmt3b promotes DNA methylation along the body of the enhancer. Depletion of either protein inactivates their target enhancers and profoundly affects epidermal stem cell function. Altogether, we reveal novel functions for Dnmt3a and Dnmt3b at enhancers that could contribute to their roles in disease and tumorigenesis.

Introduction

Establishing cell fates during development depends on *de novo* DNA methylation catalyzed by Dnmt3a and Dnmt3b (Okano et al., 1999; Wu and Zhang, 2014). Both proteins also play important roles in adult tissue homeostasis (Challen et al., 2014; Rinaldi and Benitah, 2014; Wu et al., 2010), and their deregulation is causative of disease, including tumorigenesis (Timp and Feinberg, 2013). Depletion of the DNA methyltransferases Dnmt3a, Dnmt3b, or Dnmt1 perturbs the homeostasis of several tissues, including the epidermis, hematopoietic cells, lung, intestine, and neural cells (Broske et al., 2009; Challen et al., 2014; 2012; Sheaffer et al., 2014; Trowbridge et al., 2009). Naturally occurring somatic mutations in Dnmts can drive hematologic malignancies and are causative of a diseased state (Rinaldi and Benitah, 2014; Shaffer et al., 2014; Shlush et al., 2014; Sun et al., 2014). Interpreting these phenotypes has been hampered by the lack of information regarding the genomic localization of each endogenous protein in adult tissues.

Here we studied the role of endogenous Dnmt3a and Dnmt3b during human epidermal stem cell (EpSC) differentiation. Expression of the maintenance DNA methyltransferase Dnmt1 is high in the basal cells of the epidermis and decreases as the basal cells differentiate, leading to a decrease in the content and amplitude of DNA methylation in differentiated keratinocytes as compared to epidermal basal cells (Sen et al., 2010). Dnmt1-deficient human EpSCs undergo premature and irreversible differentiation (Sen et al., 2010), although it is not known to what extent this effect is dependent on changes in DNA methylation. Intriguingly, conditional Dnmt1 deletion in mouse epidermis only results in uneven epidermal thickness and a reduction of the hair follicle length during ageing (Li et al., 2012). While genome-wide single-base

pair resolution analysis of DNA methylation revealed similar patterns between quiescent and active proliferating hair follicle stem cells in young mice (Bock et al., 2012), it also identified more than 2,000 differentially methylated regions. If and how *de novo* DNA methyltransferases regulate the function of EpSCs and their differentiated counterparts is unknown. We now reveal that Dnmt3a and Dnmt3b have previously unidentified functions through their association with distal transcriptional regulatory elements during EpSC homeostasis.

Results

Dnmt3a and Dnmt3b are Differentially Expressed During Human EpSC Differentiation

To study the dynamics of EpSC differentiation, we have previously monitored the stepwise changes in gene expression during differentiation every five hours for two consecutive days (Janich et al., 2013; Luis et al., 2011; Sen et al., 2010). Expression of stem cells and differentiation markers followed the expected pattern during differentiation (Toufighi et al., 2015). The *de novo* DNA methyltransferases Dnmt3a and Dnmt3b were highly expressed in EpSCs, but Dnmt3a increased during differentiation, while Dnmt3b diminished at the onset of differentiation (Figure S1A–B and Table S1A).

Dnmt3a and Dnmt3b Dynamically Bind to the Most Active Enhancers During EpSC Differentiation

To study whether expression changes in the *de novo* DNA methyltransferases during EpSC differentiation are functionally relevant, we performed ChIP-seq of both endogenous proteins in two biological replicates (Figures 1 and S1C). The Pearson

correlation coefficients for the biological replicates were 0.72 and 0.89 for Dnmt3a and Dnmt3b, respectively (Table S2A). Using DeSeq2 as a stringent statistical method to measure differential binding, we observed that Dnmt3a occupied more sites, and Dnmt3b fewer sites, during stem cell differentiation, mirroring their expression pattern during differentiation (Figure S1C and Table S2B). MACS-peak calling revealed that, of the peaks common between stem cells and differentiated states, 68% of Dnmt3a peaks significantly increased in amplitude during differentiation, while 75% of Dnmt3b peaks decreased (Figure S1D). Thus, genomic sites occupied by Dnmt3a increase, and those occupied by Dnmt3b decrease, during human EpSC differentiation.

Genomic localization of the two proteins showed little overlap, suggesting they have specific and dynamic functions (Table S2B). To better map these distinct genomic locations, we performed ChIP-seq in stem cells and differentiated cells for H3K4me3 (for active promoters), H3K4me1 (for enhancers), H3K27ac (for active enhancers and transcribed genes), methylated DNA (using MeDIP and whole genome bisulfite sequencing), and hydroxymethylated DNA (hMeDIP) (Figure S1F and Table S3A). We also analyzed both cell states with RNA-seq to correlate the genomic localization of Dnmt3a and Dnmt3b with changes in their gene expression (Figure S1E).

A significant proportion of the genomically-bound Dnmt3a and Dnmt3b was located at intergenic regions (Figures 1A–D and Table S2B). These sites are rich in H3K4me1 and H3K27ac, which define enhancers (Figure 1A). Enhancers promote distal gene expression by physically connecting with their promoters. Dynamic changes in enhancer activity regulate the expression of cell fate genes during development (Hon

et al., 2013; Smith and Shilatifard, 2014). They can be either poised (H3K4me1-positive) or active (H3K4me1/H3K27ac–double positive) and produce bidirectional enhancer RNAs (eRNAs) that stabilize the interactive loop with promoters (Kim and Shiekhattar, 2015; Lai and Shiekhattar, 2014). We first analyzed enhancer behavior during human EpSC differentiation with ChIP-seq analysis of H3K4me1 and H3K27ac in three biological triplicates of EpSCs and their differentiated counterparts (Figure S1G). DeSeq2 showed that the majority (76%) of active enhancers in human EpSCs are significantly decommissioned during differentiation (Figure S1H and Table S3B). Strikingly, 11,825 enhancers were enriched exclusively in the stem cell state; proximity analysis suggested that these enhancers drove the expression of genes that define the ectoderm lineage—and therefore functionality—of stem cells, such as *ITGA6, TP63, KRT5,* and *KRT14* (Figure S1H). Upon terminal differentiation, 110 enhancers were activated *de novo*; those enhancers are associated to epidermal differentiation genes such as involucrin, cornifin, and other members of Epidermal Differentiation Complex (Figure S1H and Table S3C). Thus, enhancers are very dynamic during the linear transition of EpSCs towards differentiated keratinocytes (Cavazza et al., 2016).

Intriguingly, both Dnmt3a and Dnmt3b were predominantly located at active enhancers (Figure 1A–D). Dnmt3a displayed sharp peaks at the center of its target enhancers, whereas Dnmt3b had broader peaks that occupied the enhancer center and body (Figures 1A, 1B, 2C, and 2D). Enhancers can be subclassified as two types: typical enhancers, which are bound by a small number of transcription factors and contain sharp peaks of H3K4me1 and H3K27ac, and super-enhancers (SEs), which span approximately 20 kb and are cobound by several transcription factors (Hnisz et

al., 2013). SEs define the pluripotency network in embryonic stem cells and the corresponding cellular fate in adult tissues (Hnisz et al., 2013). Based on the size distribution of H3K27ac, we identified 12,930 active typical enhancers, and 315 intergenic SEs, in human EpSCs (Figure 1E). Dnmt3a occupied 981, and Dnmt3b, 497, typical enhancers. However, both proteins preferred large, distal regulatory SE domains (Figure 1F and Table S4A). Enhancers bound by Dnmt3a or Dnmt3b expressed significantly higher levels of enhancer RNAs and their associated mRNAs than enhancers not bound by either protein (Figure 1G and Table S4B). Still, the positive correlation between eRNA and mRNA levels and Dnmt3 binding was more pronounced with Dnmt3b than Dnmt3a. Gene ontology (GO) based on proximity analysis indicated that, in stem cells, SEs with either Dnmt3a or Dnmt3b regulated genes involved in cell proliferation, keratinocyte fate, epidermal morphogenesis, or adhesion of stem cells to their ECM (Figures S1I and SJ), while those with Dnmt3a in differentiated keratinocytes were related to genes predominantly involved in epidermal differentiation (Figure S1J).

Dnmt3a and Dnmt3b are Recruited to Active Enhancers in an H3K36me3-Dependent Manner

The PWWP domain of Dnmt3a and Dnmt3b interacts with H3K36me3, a chromatin mark associated to transcriptional elongation, to bind to gene bodies (Baubec et al., 2015; Dhayalan et al., 2010; Morselli et al., 2015; Rondelet et al., 2016). Although H3K36me3 is differentially enriched at active enhancers, correlating with enhancer activity (Zetner et al., 2011), its role at these regulatory regions is not known. Indeed, ChIP-seq of H3K36me3 in human EpSCs indicated that enhancers bound by Dnmt3a or Dnmt3b contained significantly higher levels H3K36me3 than the cohort of active

enhancers not bound by either protein (Figure 2A). Knockdown of the methyltransferase Setd2, which methylates H3K36, strongly reduced the localization of Dnmt3a and Dnmt3b to their respective target enhancers (Figure 2B–D). Thus, Dnmt3a and Dnmt3b may require H3K36 trimethylation to bind to their target enhancers.

To test how Dnmt3a and Dnmt3b bind their target enhancers, we first infected primary human keratinocytes with a RFP lentiviral inducible shRNA against endogenous Dnmt3a and Dnmt3b (Figure 2E). After the endogenous proteins were knocked down, cells were infected with a retroviral vector expressing GFP and a wild-type version of Dnmt3a1 or Dnmt3b1 (the most abundant isoforms expressed in human EpSCs) (Table S1A), or with a mutanted PWWP domain unable to bind to H3K36me3 (Baubec et al., 2015; Chen et al., 2004). Double RFP/GFP–positive cells were then FACS-sorted and analyzed by ChIP-qPCR for Dnmt3a or Dnmt3b binding at target enhancers (Figure 2E). Wild-type versions, but not the PWWP mutants, efficiently bound their target enhancers, indicating that both proteins directly interact with these regulatory elements by associating with H3K36me3 through the PWWP domain (Figure 2E). We confirmed that the Dnmt3b-PWWP mutant could no longer bind to gene bodies, as previously reported for mouse embryonic stem cells (Baubec et al., 2015) (Figure 2E). Conversely, the Dnmt3A1-PWWP mutant bound its target promoters, which are devoid of H3K36me3 (Figures 2E and Table S1). Wild-type and PWWP mutants of Dnmt3a and Dnmt3b were expressed at equal levels (Figure 2F).

Dnmt3a Interacts with p63 to Associate to its Target Enhancers

As Dnmt3a binds to the center of the enhancers, we next asked whether it functionally interacts with specific transcription factors to regulate enhancer activity. A transcription factor binding motif search revealed that enhancers bound by Dnmt3a were enriched for AP1, p63, TCF3, and MYC motifs (Figure 2G). p63, a master regulator of the ectodermal fate, interacts with enhancers to regulate a gene expression program required for epidermal homeostasis (Kouwenhoven et al., 2015) (Figure 2H). Similar to Dnmt3a, p63 showed a preference for SEs, both in stem cell and differentiated states (Kouwenhoven et al., 2015). Approximately 50% of the Dnmt3a-associated enhancers were bound by p63 in EpSCs, which corresponded to those regulating the expression of genes involved in keratinocyte proliferation and identity (Figure 2I).

Immunoprecipitation studies indicated that both endogenous proteins directly interact in primary human keratinocytes (Figure 2J). p63 depletion significantly reduced the localization of Dnmt3a at numerous target enhancers, as determined by ChIP-qPCR (Figures 2K–2L). Thus, Dnmt3a and p63 physically and functionally interact at enhancers to regulate EpSC function.

Dnmt3a and Tet2 Maintain 5-hmC at Active Enhancers in Human EpSCs

In EpSCs, enhancers bound by Dnmt3a were always within a valley of DNA methylation yet contained high levels of DNA hydroxymethylation, as compared to those bound by Dnmt3b or not bound by either protein (Figures 3A-B). In addition, enhancers decorated by Dnmt3a during EpSC differentiation acquired higher levels of 5-hydroxymethylcytosine (5-hmC) (Figure S2A–B). Knockdown of Dnmt3a significantly and specifically reduced 5-hmC levels at the center of its target

enhancers, but had no effect on 5-hmC levels at enhancers bound by Dnmt3b or not bound by Dnmt3a (Figure 3B). Dnmt3a could promote the methylation of its target enhancers, which are then hydroxymethylated to permit their active state. To test this, we first verified that only Tet2 (of the three Tet proteins that catalyze DNA hydroxymethylation) was highly expressed in human EpSCs (Table S1A). We then tested whether Tet2 depletion would reveal the DNA methylation deposited by Dnmt3a at its target enhancers. Complete Tet2 depletion severely compromised EpSC viability (data not shown). Cells tolerated a 50% knockdown of Tet2 expression (Figure S2D), which also slightly but significantly increased the level of DNA methylation uniquely at the Dnmt3a-bound, but not Dnmt3b-bound or unbound, enhancers (Figures 3C–3D).

To determine whether the methyltransferase domain of Dnmt3a was important for the hydroxymethylation of its target enhancers, we depleted primary keratinocytes of endogenous Dnmt3a, ectopically expressed either wild-type Dnmt3a1 or a methyltransferase dead mutant (methyl mut), and then measured the levels of 5-hmC at Dnmt3a target enhancers (Chen et al., 2004) (Figures 3E and S4C). Indeed, overexpression of Dnmt3a promoted EpSC differentiation, as determined by a reduced clonogenic potential and an increased expression of terminal differentiation genes (Figures 3E, 3F, S1A, and S1B). Following ectopic expression of Dnmt3a, we measured the levels of 5-hmC at those Dnmt3a-bound enhancers in differentiated keratinocytes. Loss of endogenous Dnmt3a reduced 5-hmC levels at these enhancers, further confirming our hMeDIP-seq results (Figure 3E). Importantly, only ectopically expressed wild-type Dnmt3a, but not the methyltransferase mutant, rescued the loss of 5-hmC induced by knockdown of endogenous Dnmt3a (Figure 3E). Overexpression

of the methyltransferase mutant failed to induce epidermal differentiation, further indicating that the catalytic domain of Dnmt3a is essential for its function in epidermal cells (Figures 3E-F). Thus, these results strongly suggest that Dnmt3a and Tet2 cooperate to subsequently induce DNA methylation and hydroxymethylation of enhancers to regulate EpSCs homeostasis.

Dnmt3b Promotes DNA Methylation Along Active Enhancers

Dnmt3b binding to the enhancer body correlated with higher levels of DNA methylation and lower levels of DNA hydroxymethylation as compared to the Dnmt3a-bound enhancers or those bound by neither protein (Figures 3B and 3H). Dnmt3b depletion in EpSCs had no effect on DNA hydroxymethylation at or around its target enhancers (Figure 3B) but significantly lowered the amount of DNA methylation along the enhancer (Figure 3I), reminiscent of the known role of Dnmt3b in gene body methylation. This effect was not observed after Dnmt3a knockdown (Figure 3I). Dnmt3b is recruited to gene bodies in different cell types and promotes genic DNA methylation in a manner dependent on histone H3K36me3 (Baubec et al., 2015; Mikkelsen et al., 2007; Morselli et al., 2015). Our results show that Dnmt3b spanned the entire gene body of a specific group of genes in EpSCs as well (Figures S3A–S3C). These large domains of Dnmt3b significantly correlated with high mRNA expression and broad areas of genic H3K4me3, which confer transcriptional consistency and robustness (Benayoun et al., 2014) (Figures S3B and S3C). These genes defined the stem cell signature in EpSCs as well as the differentiated signature in differentiated keratinocytes (Figure S3E and Table S4C). In general, broad genic occupancy by Dnmt3b correlated with high levels of gene body DNA methylation

(Figure S3F), and Dnmt3b depletion significantly reduced genic DNA methylation (Figure S3G).

Depletion of Setd2, the methyltransferase that deposits H3K36me3, significantly reduced binding of Dnmt3b to gene bodies and to enhancers (Figures 3G, S3H, and S3I). Hence, Dnmt3b is required to promote gene body and enhancer body DNA methylation, which correlates to transcription of both regions.

Dnmt3a and Dnmt3b Promote Enhancer Activity and are Required for Human EpSC Homeostasis

Changes in DNA methylation or hydroxymethylation caused by knockdown of Dnmt3b or Dnmt3a, respectively, correlated with reduced enhancer activity, as measured by transcribed enhancer RNA levels, as well as reduced H3K27ac levels (Figures 4A–4C and Table S4D). This effect was observed in typical enhancers and SEs bound by Dnmt3a or Dnmt3b (Figures 4A–4C). For instance, Dnmt3a and Dnmt3b associated with an intragenic enhancer recently identified to drive the expression of ΔNp63 (Antonini et al., 2015), and their depletion in EpSCs also decreased the activity of a luciferase reporter containing it (Figures S2C). Specificity of Dnmt3a or Dnmt3b binding to enhancers was confirmed in Dnmt3a- or Dnmt3b-depleted stem cells by ChIP-seq (Figure S2E).

We next asked whether modulating the expression of either Dnmt3a or Dnmt3b affects self-renewal and/or differentiation of EpSCs. Dnmt3b predominantly associates to enhancers and gene bodies of genes involved in the self-renewal and interaction of EpSCs with their niche; differentiation reduces its expression and

genomic binding. Dnmt3a positively regulates expression of genes involved in stem cell proliferation, and interacts with the extracellular matrix via its association with enhancers. Upon epidermal differentiation, its genomic binding shifts to activate enhancers that promote expression of genes that drive epidermal differentiation. We first performed an *in vivo* competition assay between primary human keratinocytes, depleted or not for Dnmt3a or Dnmt3b, that had been transplanted into immunocompromised mice; keratinocytes were GFP-tagged, and the shRNA vectors were RFP tagged (Figure 4D). Four weeks after transplanting, GFP-positive cells and RFP-shControl cells contributed equally to all layers of the reconstituted epithelium. However, Dnmt3a-KD and Dnmt3b-KD cells barely contributed to the basal layer and were predominantly detected in the differentiated strata of the epithelium (Figure 4E). Furthermore, knockdown of either protein impaired the self-renewing potential of human EpSCs, as determined by a significant reduction in their clonogenic potential in culture (Figures 4F, S4A, and S4B). These changes were accompanied by an increased expression of genes involved in epidermal terminal differentiation, and a decreased expression of those involved in stem cell proliferation and adhesion to the ECM (Figures 4G–4I and Table S4D). Expressions of genes closest to the enhancers bound by Dnmt3a/3b were affected by depletion of Dnmt3a/3b (Figure 4H). EpSCs depleted of Dnmt3a or Dnmt3b differentiated in the absence of any pro-differentiation stimulus. However, Dnmt3a expression increases during epidermal differentiation (Figures S1A-B), and ectopic expression of wild-type Dnmt3a1 induced spontaneous differentiation in EpSCs (Figure 3E). Dnmt3a genomic localization shifted from enhancers that regulate the expression of genes involved in stem cell proliferation to those that regulate differentiation genes. Driving EpSCs to differentiate by raising the calcium concentration in the medium led to those depleted

of Dnmt3a—but not of Dnmt3b—to express lower levels of epidermal differentiation markers than differentiating control cells (Figure 4J). Thus, Dnmt3a has a dual role in maintaining EpSC self-renewal, while also promoting differentiation once basal cells have committed to differentiate.

Discussion

We determined that Dnmt3a and Dnmt3b positively regulate gene expression through non-overlapping functions at regulatory elements via distinct mechanisms. Dnmt3b promotes methylation not only at genes but also at enhancer body DNA, both of which are required to sustain high transcriptional activity of mRNA or eRNA, respectively (Hon et al., 2013; Rasmussen et al., 2015). Interestingly, enhancer RNAs increase the association of transcription factors with enhancers (Sigova et al., 2015). Hence, the positive impact of Dnmt3a and Dnmt3b on the production of enhancer RNAs might contribute to the overall robustness of enhancer activity.

Dnmt3a/b recruitment to enhancers depends on the presence of H3K36me3. Intriguingly, Dnmt3a requires p63 to bind to its target enhancers. It remains to be determined how and why Dnmt3a and Dnmt3b preferentially associate to some enhancers, and to some gene bodies, at the genome-wide scale. For instance, Dnmt3a decorates gene bodies of neurogenesis genes in murine neural stem cells, whereas Dnmt3b (but not Dnmt3a) interacts with gene bodies in murine and human embryonic stem cells (Wu et al., 2010).

We also observed the same pattern of Dnmt3a and Dnmt3b genomic localization at enhancers, and of Dnmt3b at gene bodies, in primary human dermal fibroblasts,

indicating that their interaction with enhancers is likely to be a general function in somatic cells (Figures S4D). However, there was virtually no overlap between the enhancers bound by either protein, nor the genes and biological functions regulated by these, in human primary fibroblasts or human EpSCs, further indicating that their specific genomic localization is highly influenced by the cellular context (Figures S4E–S4G). Considering that deregulation of Dnmt3a and Dnmt3b affects tumourigenesis in several tissues (Timp and Feinberg, 2013; Witte et al., 2014), these newly identified functions might have important roles in regulating the homeostasis and tumour development of these different tissues.

References

Antonini, D., Sirico, A., Aberdam, E., Ambrosio, R., Campanile, C., Fagoonee, S., Altruda, F., Aberdam, D., Brissette, J.L., and Missero, C. (2015). A composite enhancer regulates p63 gene expression in epidermal morphogenesis and in keratinocyte differentiation by multiple mechanisms. Nucleic Acids Res *43*, 862–874.

Baubec, T., Colombo, D.F., Wirbelauer, C., Schmidt, J., Burger, L., Krebs, A.R., Akalin, A., and Schubeler, D. (2015). Genomic profiling of DNA methyltransferases reveals a role for DNMT3B in genic methylation. Nature.

Benayoun, B.A., Pollina, E.A., Ucar, D., Mahmoudi, S., Karra, K., Wong, E.D., Devarajan, K., Daugherty, A.C., Kundaje, A.B., Mancini, E., et al. (2014). H3K4me3 breadth is linked to cell identity and transcriptional consistency. Cell *158*, 673–688.

Bock, C., Beerman, I., Lien, W.-H., Smith, Z.D., Gu, H., Boyle, P., Gnirke, A., Fuchs, E., Rossi, D.J., and Meissner, A. (2012). DNA methylation dynamics during in vivo differentiation of blood and skin stem cells. Mol Cell *47*, 633–647..

Broske, A.-M., Vockentanz, L., Kharazi, S., Huska, M.R., Mancini, E., Scheller, M., Kuhl, C., Enns, A., Prinz, M., Jaenisch, R., et al. (2009). DNA methylation protects hematopoietic stem cell multipotency from myeloerythroid restriction. Nat Genet *41*, 1207–1215.

Cavazza, A., Miccio, A., Romano, O., Petiti, L., Malagoli Tagliazucchi, G., Peano, C., Severgnini, M., Rizzi, E., De Bellis, G., Bicciato, S., et al. (2016). Dynamic Transcriptional and Epigenetic Regulation of Human Epidermal Keratinocyte Differentiation. Stem Cell Reports *6*, 618–632.

Challen, G.A., Sun, D., Jeong, M., Luo, M., Jelinek, J., Berg, J.S., Bock, C., Vasanthakumar, A., Gu, H., Xi, Y., et al. (2012). Dnmt3a is essential for

hematopoietic stem cell differentiation. Nat Genet *44*, 23–31.

Challen, G.A., Sun, D., Mayle, A., Jeong, M., Luo, M., Rodriguez, B., Mallaney, C., Celik, H., Yang, L., Xia, Z., et al. (2014). Dnmt3a and Dnmt3b have overlapping and distinct functions in hematopoietic stem cells. Cell Stem Cell *15*, 350–364.

Chen, T., Tsujimoto, N., and Li, E. (2004). The PWWP domain of Dnmt3a and Dnmt3b is required for directing DNA methylation to the major satellite repeats at pericentric heterochromatin. Mol Cell Biol *24*, 9048–9058.

Dhayalan, A., Rajavelu, A., Rathert, P., Tamas, R., Jurkowska, R.Z., Ragozin, S., and Jeltsch, A. (2010). The Dnmt3a PWWP domain reads histone 3 lysine 36 trimethylation and guides DNA methylation. J Biol Chem *285*, 26114–26120.

Hnisz, D., Abraham, B.J., Lee, T.I., Lau, A., Saint-Andre, V., Sigova, A.A., Hoke, H.A., and Young, R.A. (2013). Super-enhancers in the control of cell identity and disease. Cell *155*, 934–947.

Hon, G.C., Rajagopal, N., Shen, Y., McCleary, D.F., Yue, F., Dang, M.D., and Ren, B. (2013). Epigenetic memory at embryonic enhancers identified in DNA methylation maps from adult mouse tissues. Nat Genet *45*, 1198–1206.

Janich, P., Toufighi, K., Solanas, G., Luis, N.M., Minkwitz, S., Serrano, L., Lehner, B., and Benitah, S.A. (2013). Human epidermal stem cell function is regulated by circadian oscillations. Cell Stem Cell *13*, 745–753.

Kim, T.-K., and Shiekhattar, R. (2015). Architectural and Functional Commonalities between Enhancers and Promoters. Cell *162*, 948–959.

Kouwenhoven, E.N., Oti, M., Niehues, H., van Heeringen, S.J., Schalkwijk, J., Stunnenberg, H.G., van Bokhoven, H., and Zhou, H. (2015). Transcription factor p63 bookmarks and regulates dynamic enhancers during epidermal differentiation. EMBO Rep *16*, 863–878.

Lai, F., and Shiekhattar, R. (2014). Enhancer RNAs: the new molecules of transcription. Curr Opin Genet Dev *25*, 38–42.

Li, J., Jiang, T.-X., Hughes, M.W., Wu, P., Yu, J., Widelitz, R.B., Fan, G., and Chuong, C.-M. (2012). Progressive alopecia reveals decreasing stem cell activation probability during aging of mice with epidermal deletion of DNA methyltransferase 1. J Invest Dermatol *132*, 2681–2690.

Luis, N.M., Morey, L., Mejetta, S., Pascual, G., Janich, P., Kuebler, B., Cozutto, L., Roma, G., Nascimento, E., Frye, M., et al. (2011). Regulation of human epidermal stem cell proliferation and senescence requires polycomb- dependent and -independent functions of Cbx4. Cell Stem Cell *9*, 233–246.

Mikkelsen, T.S., Ku, M., Jaffe, D.B., Issac, B., Lieberman, E., Giannoukos, G., Alvarez, P., Brockman, W., Kim, T.-K., Koche, R.P., et al. (2007). Genome-wide maps of chromatin state in pluripotent and lineage-committed cells. Nature *448*, 553–560.

Morey, L., Pascual, G., Cozzuto, L., Roma, G., Wutz, A., Benitah, S.A., and Di Croce, L. (2012). Nonoverlapping functions of the Polycomb group Cbx family of proteins in embryonic stem cells. Cell Stem Cell *10*, 47–62.

Morselli, M., Pastor, W.A., Montanini, B., Nee, K., Ferrari, R., Fu, K., Bonora, G., Rubbi, L., Clark, A.T., Ottonello, S., et al. (2015). In vivo targeting of de novo DNA methylation by histone modifications in yeast and mouse. Elife *4*, e06205.

Okano, M., Bell, D.W., Haber, D.A., and Li, E. (1999). DNA methyltransferases Dnmt3a and Dnmt3b are essential for de novo methylation and mammalian development. Cell *99*, 247–257.

Rasmussen, K.D., Jia, G., Johansen, J.V., Pedersen, M.T., Rapin, N., Bagger, F.O., Porse, B.T., Bernard, O.A., Christensen, J., and Helin, K. (2015). Loss of TET2 in hematopoietic cells leads to DNA hypermethylation of active enhancers and induction of leukemogenesis. Genes Dev *29*, 910–922.

Rinaldi, L., and Benitah, S.A. (2014). Epigenetic regulation of adult stem cell function. Febs J.

Rondelet, G., Dal Maso, T., Willems, L., and Wouters, J. (2016). Structural basis for recognition of histone H3K36me3 nucleosome by human de novo DNA methyltransferases 3A and 3B. J Struct Biol.

Sen, G.L., Reuter, J.A., Webster, D.E., Zhu, L., and Khavari, P.A. (2010). DNMT1 maintains progenitor function in self-renewing somatic tissue. Nature *463*, 563–567.

Shaffer, B., McGraw, S., Xiao, S.C., Chan, D., Trasler, J., and Chaillet, J.R. (2014). The Dnmt1 Intrinsically Disordered Domain Regulates Genomic Methylation During Development. Genetics.

Sheaffer, K.L., Kim, R., Aoki, R., Elliott, E.N., Schug, J., Burger, L., Schubeler, D., and Kaestner, K.H. (2014). DNA methylation is required for the control of stem cell differentiation in the small intestine. Genes Dev *28*, 652–664.

Shlush, L.I., Zandi, S., Mitchell, A., Chen, W.C., Brandwein, J.M., Gupta, V., Kennedy, J.A., Schimmer, A.D., Schuh, A.C., Yee, K.W., et al. (2014). Identification of pre-leukaemic haematopoietic stem cells in acute leukaemia. Nature *506*, 328–333.

Sigova, A.A., Abraham, B.J., Ji, X., Molinie, B., Hannett, N.M., Guo, Y.E., Jangi, M., Giallourakis, C.C., Sharp, P.A., and Young, R.A. (2015). Transcription factor trapping by RNA in gene regulatory elements. Science.

Smith, E., and Shilatifard, A. (2014). Enhancer biology and enhanceropathies. Nat Struct Mol Biol *21*, 210–219.

Sun, Z., Wu, Y., Ordog, T., Baheti, S., Nie, J., Duan, X., Hojo, K., Kocher, J.-P., Dyck, P.J., and Klein, C.J. (2014). Aberrant signature methylome by DNMT1 hot spot mutation in hereditary sensory and autonomic neuropathy 1E. Epigenetics *9*, 1184–1193.

Timp, W., and Feinberg, A.P. (2013). Cancer as a dysregulated epigenome allowing

cellular growth advantage at the expense of the host. Nat Rev Cancer *13*, 497–510.

Toufighi, K., Yang, J.-S., Luis, N.M., Aznar Benitah, S., Lehner, B., Serrano, L., and Kiel, C. (2015). Dissecting the calcium-induced differentiation of human primary keratinocytes stem cells by integrative and structural network analyses. PLoS Comput Biol *11*, e1004256.

Trowbridge, J.J., Snow, J.W., Kim, J., and Orkin, S.H. (2009). DNA methyltransferase 1 is essential for and uniquely regulates hematopoietic stem and progenitor cells. Cell Stem Cell *5*, 442–449.

Witte, T., Plass, C., and Gerhauser, C. (2014). Pan-cancer patterns of DNA methylation. Genome Med *6*, 66.

Wu, H., and Zhang, Y. (2014). Reversing DNA methylation: mechanisms, genomics, and biological functions. Cell *156*, 45–68.

Wu, H., Coskun, V., Tao, J., Xie, W., Ge, W., Yoshikawa, K., Li, E., Zhang, Y., and Sun, Y.E. (2010). Dnmt3a-dependent nonpromoter DNA methylation facilitates transcription of neurogenic genes. Science *329*, 444–448.

Author Contributions

L.R. and S.A.B. designed the experiments. L.R. performed all experiments with the help of J.S. and G.S.. D.D. and L.R performed the bioinformatics analysis of the data. L.M. performed the initial ChIP-seq of Dnmt3a and Dnmt3b. I.G. performed the strand-specific RNA-seq. ChIP-seq was performed by J.I.P. from the Genomics Unit of the IRB. L.D.C. helped to analyze all genome-wide results. L.R. and S.A.B. wrote the manuscript. Genomic data files were uploaded to the NCBI Geo database (GSE65838). The authors declare no competing financial interests.

Acknowledgements

The S.A.B. lab research is supported by the European Research Council (ERC), the Worldwide Cancer Research Foundation, the Foundation *La Marató de TV3*, the Spanish Ministry of Economy and Development, the Foundation *Vencer el Cancer* (“Beat Cancer”), the Government of Cataluña (SGR and Mario Salviá grants), the

Foundation *Fundación Botín*, and the Institute for Research in Biomedicine (IRB-Barcelona). L.R. is a La Caixa Foundation PhD fellow. G.S. was supported by an AXA postdoctoral fellowship. IRB Barcelona is the recipient of a *Severo Ochoa Award of Excellence* from MINECO (Government of Spain). L.D.C. was supported by grants from the Spanish "Ministerio de Educación y Ciencia" (SAF2013-48926-P), and the European Commission's 7th Framework Program 4DCellFate grant number 277899. We are grateful to the Common Fund´s Epigenomic Program from the NIH (USA) for providing the bisulphite whole genome sequencing data of primary human epidermal keratinocytes (https://commonfund.nih.gov/epigenomics/index). We thank all the core facilities at the IRB-Barcelona for their assistance in our work, V. Raker for manuscript editing, and C. Missero and D. Antonini for the luciferase reporter construct containing the intragenic enhancer of p63.

Figure Legends

Figure 1. Dnmt3a and Dnmt3b Bind at the Most Active Enhancers in EpSCs and Differentiated Keratinocytes. (A, B) ChIP-seq coverage depth (per bp per peak per 10 million mapped reads) of Dnmt3a/ Dnmt3b, H3K27ac, and H3K4me1 around the Dnmt3a/Dnmt3b peaks (–8 kb to +8 kb) in stem cells and differentiated keratinocytes. (C, D) Typical enhancer and super-enhancer (SE) bound by Dnmt3a or Dnmt3b. (E) Distribution of the H3K27ac signal (total reads) across all enhancers. (F) Fold-differences of Dnmt3a and Dnmt3b (total signal and density) between SEs and typical enhancers. Fold-changes refer to the ratio of the respective means between SEs and typical enhancers. (G) Boxplots depicting enhancer RNA and mRNA levels of closest genes, given in log (FPKM), for enhancers bound or not by Dnmt3a and/or Dnmt3b in stem cells and differentiated keratinocytes. p values were calculated using a Wilcoxon test; from left to right, $p = 3.5 \times 10^{-6}$, $p = 0.02$, $p < 2.2 \times 10^{-16}$, $p < 2.2 \times 10^{-16}$.

Figure 2. Dnmt3a/b are Recruited to Active Enhancers Through Their H3K36me3 Binding. (A) ChIP-seq coverage depth of H3K36me3 in stem cells around the intergenic enhancers (–8 kb to +8 kb) bound or not by Dnmt3a and/or Dnmt3b, as indicated. (B) Western blot of H3K36me3 levels in EpSCs infected with shCTRL or a shSETD2 lentiviral vector. (C) ChIP-seq signals at intergenic enhancers bound by Dnmt3a in stem cells infected with an shCTRL or shSETD2 lentiviral vector; $p < 2.2 \times 10^{-16}$. (D) ChIP-seq signals at intergenic enhancers bound by Dnmt3b, in cells infected with an shCTRL or shSETD2 lentiviral vector; $p < 2.2 \times 10^{-16}$. (E) Schema of FACS isolation of doubly-infected human EpSCs, expressing both inducible shRNAs against the 3′-UTR of Dnmt3a1 or Dnmt3b1 and the combined

ectopic expression of the wild-type (WT) or PWWP (WP→ST) mutant version. Lower panel: triplicates of Dnmt3a/b ChIP-qPCR, using 500,000 cells for each condition. Enrichment was normalized to a negative intergenic region. (F) Western blot of Dnmt3a and Dnmt3b in human EpSCs infected with empty vector (EV), WT, methyltransferase mutant, or PWWP mutant Dnmt3a or Dnmt3b-expressing vectors. (G) Transcription Factor Motif analysis using DREME online software at the intergenic enhancers bound by Dnmt3a. (H) Examples of enhancers bound both by tp63 and Dnmt3a. (I) Intersection between enhancers bound by tp63 and Dnmt3a, and relative gene ontology analysis of the associated genes to the cobound enhancers. (J) Immunoprecipitates of Dnmt3a and Dnmt3b, from total cell lysates from human EpSCs, and western blot against tp63. (K) Western blot against tp63 in shCtrl or in shtp63 human EpSCs. (L) Dnmt3a enrichment at intergenic enhancers cobound with tp63, showing ChIP qRT-PCR results in shCtrl and in shtp63 human EpSCs.

Figure 3. Dnmt3a and Tet2 Maintain High Levels of 5-hmC at Enhancers, whereas Dnmt3b Maintains High Levels of DNA Methylation Surrounding the Enhancer Center. (A) Relative methylation score (CpG count) measured around enhancers bound or not by Dnmt3a. $p < 2.2 \times 10^{-16}$. (B) Global levels of 5-hmC at enhancer center (–2 Kb, +2 Kb) quantified by HOMER software in EpSCs infected with shCTRL, shDnmt3a, or shDnmt3b, at enhancers bound by Dnmt3a, Dnmt3b, or neither. (C) 5-methylcytosine (5-mC) levels around enhancers bound by Dnmt3a in shCTRL and shTET2 EpSCs; $p < 2.2 \times 10^{-16}$. (D) 5-mC levels around enhancers not bound by Dnmt3a in shCTRL and shTET2 EpSCs. (E) Representation of clonogenic assay experiment of human EpSCs expressing WT Dnmt3a1, or a methyltransferase-dead mutant, compared to empty vector (EV). (F) Quantification of colonies from

clonogenic assay of EV, Dnmt3a1, or Dnmt3a1 methyltransferase mutant from three independent biological replicates. (G) Scheme method for FACS isolating doubly-infected human keratinocytes expressing GFP-tagged inducible shRNAs against 3′-UTR of Dnmt3a1, and ectopic expression of WT or the methyltransferase-dead mutant Dnmt3a (PC➔VD) co-expressing RFP. Lower panel: results from triplicate experiments of 5-hydroxyMedIP (for 5-hmC) qRT-PCR using 100,000 cells per condition. Enrichment was calculated by normalizing the value to *GAPDH* at TSS, a negative region for DNA methylation, and for DNA hydroxymethylation. (H) MeDIP-seq was used to determine 5-mC levels around enhancers bound or not bound by Dnmt3b. CpG methylated counts at enhancers bound or not bound by Dnmt3b ($p < 0.0001$) (right). (I) Relative methylation score measured around enhancers (–5 kb, +5 kb) in shCTRL and shDnmt3b EpSCs ($p < 0.0008$) (left), and in shCTRL and shDnmt3a EpSCs ($p = 0.08$) (right).

Figure 4. Depletion of Dnmt3a and Dnmt3b Decreases the Activity of its Target Enhancers. (A, B) Boxplots depicting the enhancer RNA levels, given as log (FPKM), from enhancers bound by Dnmt3a and Dnmt3b in wild-type and knockdown cells. p values were calculated using Wilcoxon-signed ranked test; from left to right, $p = 1.05 \times 10^{-5}$, 0.943, 0.003, and 2.3×10^{-10}. (C) Boxplots depicting levels of H3K27ac in CTRL and KD cells around typical enhancers and SEs bound by Dnmt3a (two left) and Dnmt3b (two right). p values were calculated using a two-sample Kolmogorov-Smirnov test; from left to right, $p < 2.2 \times 10^{-16}$, $p = 7.3 \times 10^{-15}$, $p = 0.00035$, $p = 0.04$; ***$p < 0.001$. (D) Schematic representation of competitive skin reconstitution assay between GFP EpSCs versus shRNA-RFPs EpSCs ($n = 3$ for each shRNA). (E) Representative GFP/RFP fluorescent confocal images of the human

reconstituted epithelia from the transplanted area of the three sets of transplants described in D. White bar represents 50 μm. Right, percentages of RFP and GFP cells in the basal layer of shCtrl or shDnmt3a/3b transplants. (F) Colony formation of Dnmt3a- or Dnmt3b-deficient EpSCs. Right, quantification (n = 4) of the colonies formed by Dnmt3a/b using two constitutive shRNA for each protein. (G) Immunofluorescence of involucrin, integrin α6, Dnmt3a, or Dnmt3b in shCTRL and shDnmt3a/3B EpSCs. (H) Boxplots depicting mRNA expression (from three independent biological replicates) of closest genes to enhancers bound by Dnmt3a in shCtrl and in shDnmt3a human EpSCs (left), and of closest genes to enhancers bound by Dnmt3b in shCtrl and shDnmt3b cells (right): p values were calculated using a Wilcoxon signed-ranked test; left, $p < 2.2 \times 10^{-16}$; right, $p = 7.8 \times 10^{-13}$. (I) GO analysis of genes downregulated (left) or upregulated (right) in shDnmt3a or in shDnmt3b EpSCs. (J) Relative mRNA expression levels of differentiation markers in control cells and shDnmt3a and shDnmt3b during keratinocytes differentiation. Expression levels were normalized to the housekeeping gene PUM1.

METHODS

ChIP-seq

ChIP was performed as previously described (Morey et al., 2012). Keratinocytes were trypsinized and crosslinked in 1% formaldehyde for 10 min at room temperature. To immunoprecipitate transcription factors, 2 mg of protein and 100 μg of immunoprecipitated histone/histone modifications were used. Antibodies (10 μg for Dnmt3a/3b and 3 μg for histone modifications) were incubated overnight with chromatin in ChIP buffer. Immunocomplexes were recovered with 30 μl of protein A bead slurry (Healthcare, 17-5280-01). Antibodies used for ChIP or MedIP were Dnmt3a (SantaCruz H-295), Dnmt3b (Novus Biotechnology, NB100-266), H3K27ac (Merck Millipore, 07-360), H3K4me1 (Abcam, ab8895), and H3K4me3 (Diagenode, C15410003-50), and H3K36me3 (Abcam, ab9050). Libraries for sequencing were prepared using NEBNext Ultra DNA Library Prep Kit for Illumina (E7370L) following manufacturer's instructions.

MeDIP and hMeDIP Sequencing

Purified genomic DNA (500 ng) was sonicated to obtain fragments of 300–700 bp. Adaptors from the NEBNext Ultra DNA Library Prep Kit for Illumina were added to the fragmented DNA. Fragmented DNA was incubated 2 hr with 1 μg of 5-methylcytosine (Eurogentec, BI-MECY-0100) or 5-hmC (Active Motif, 39769). Immunocomplexes were recovered using 8 μl of Dynabeads Protein A (Life Technologies) for 2 hr. Amplified libraries were prepared using NEBNext Ultra DNA Library Prep Kit for Illumina (E7370L) following manufacturer's instructions.

Figure

Figure 1

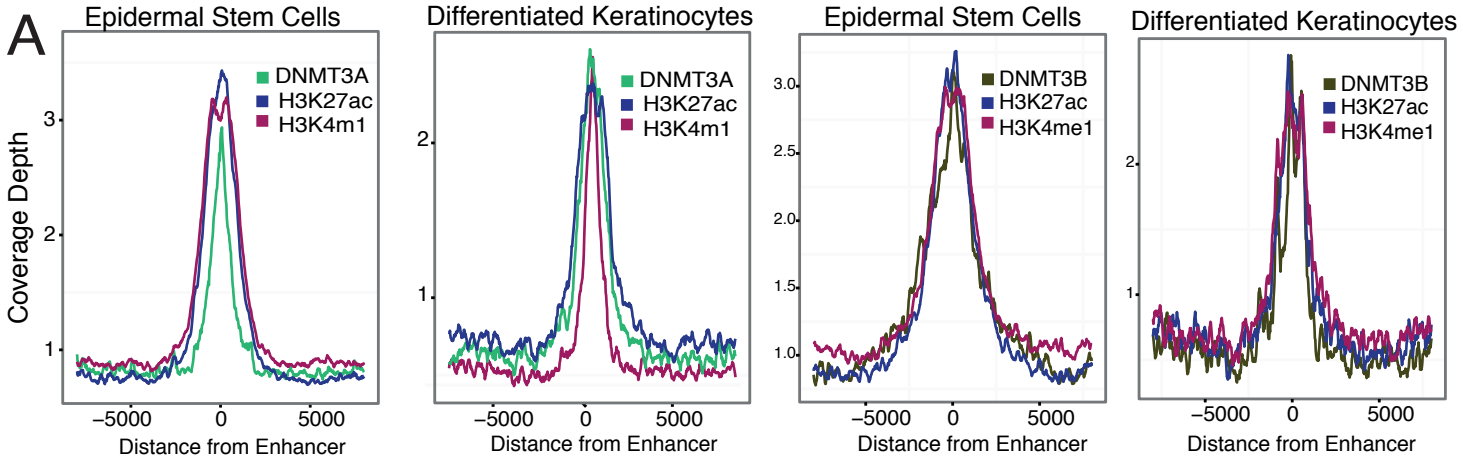

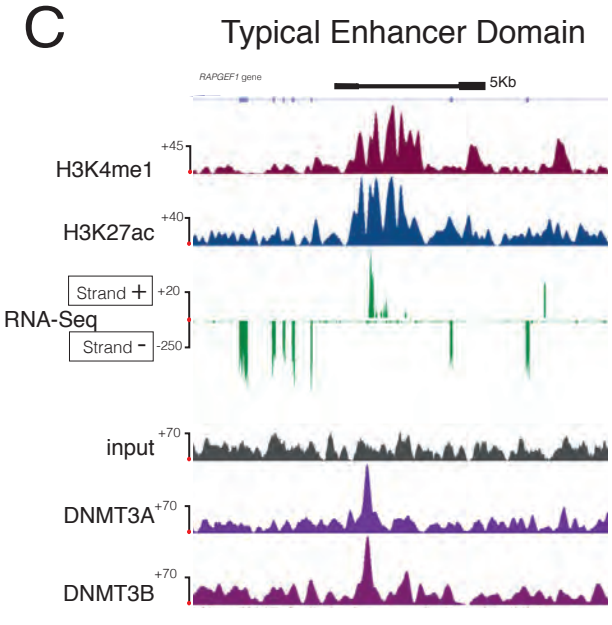

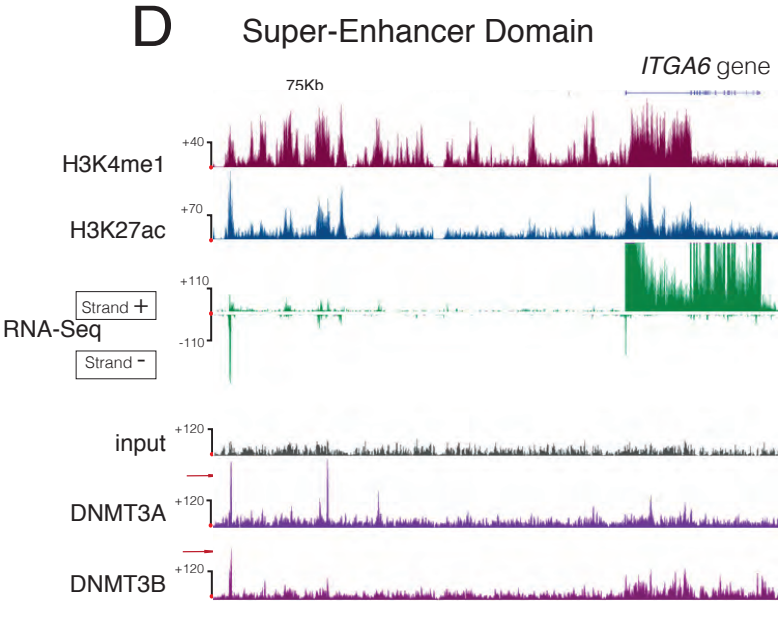

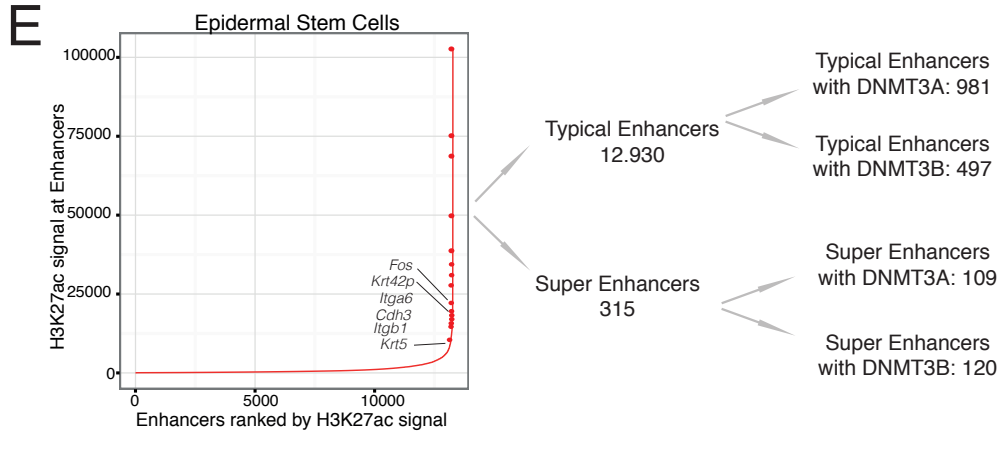

F

	Typical		Super	
	Total Signal	Density	Total Signal	Density
DNMT3A:	1X	1X	22.8X	3X
DNMT3B:	1X	1X	27.7X	3X

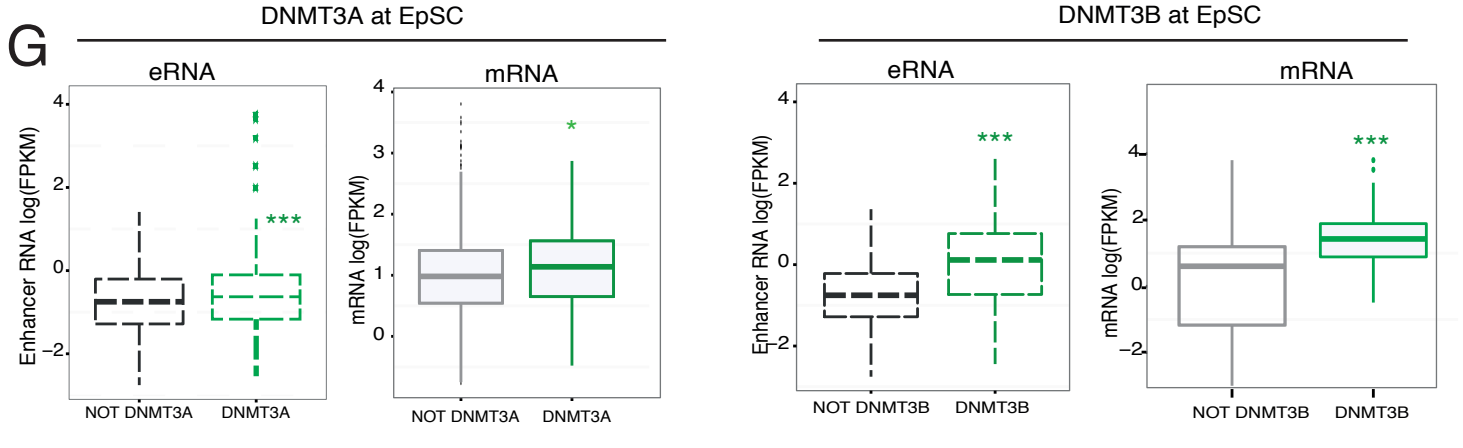

Figure

Figure 2

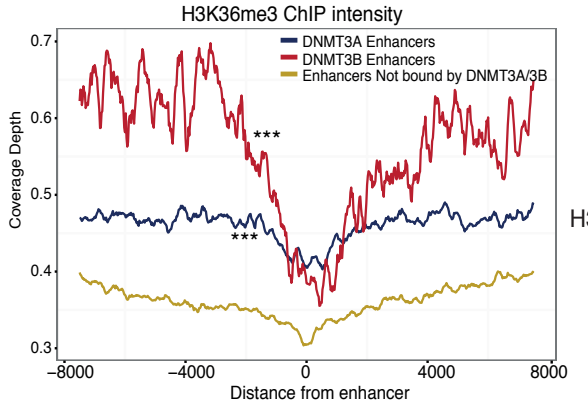

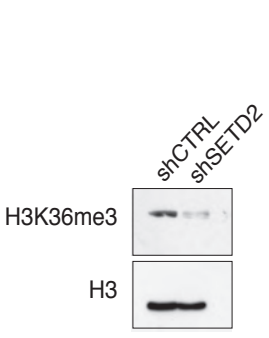

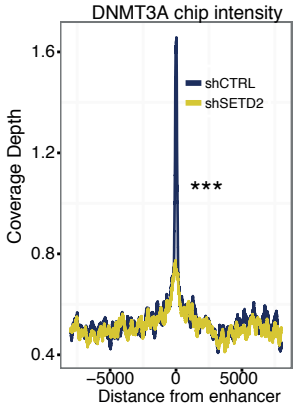

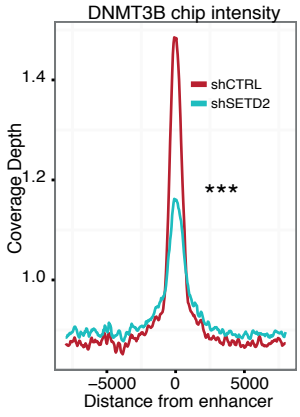

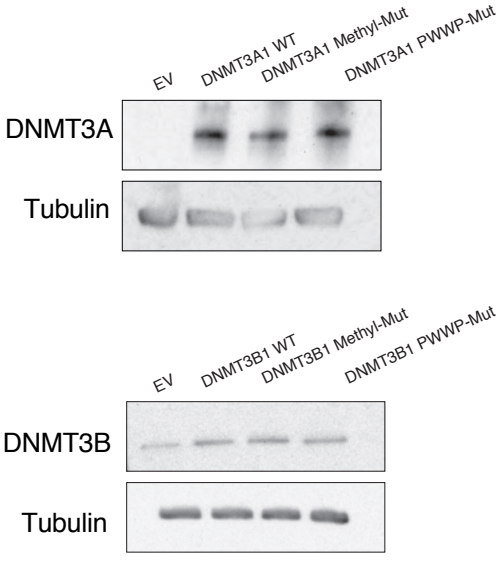

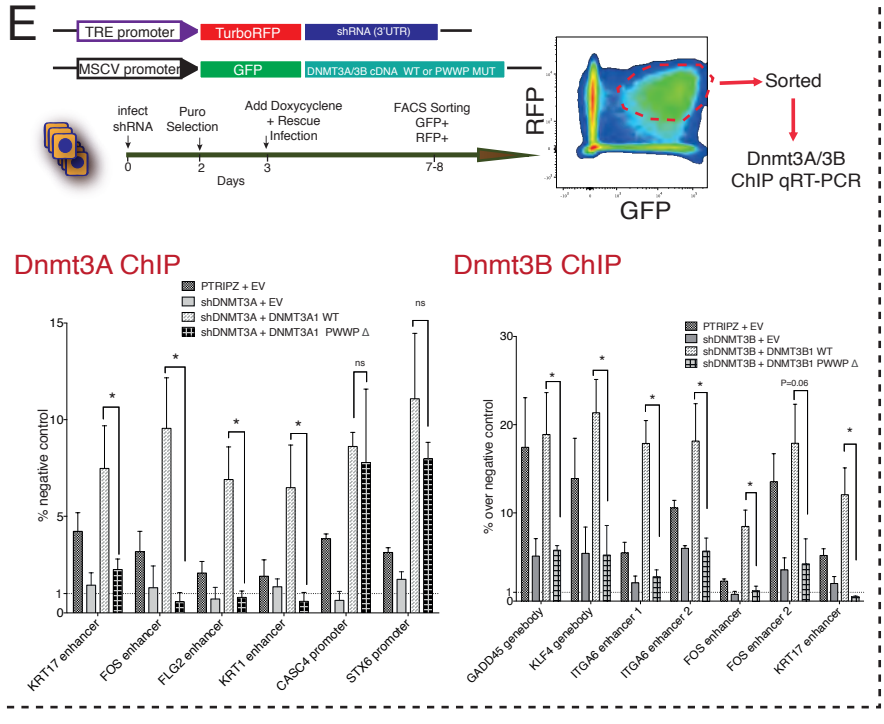

G

Transcription Factor	Motif	P-value
JUN::FOS		3.18e-77
TP63		1.64e-25
TCF3		4.05e-16
MYC		2.23e-10

H

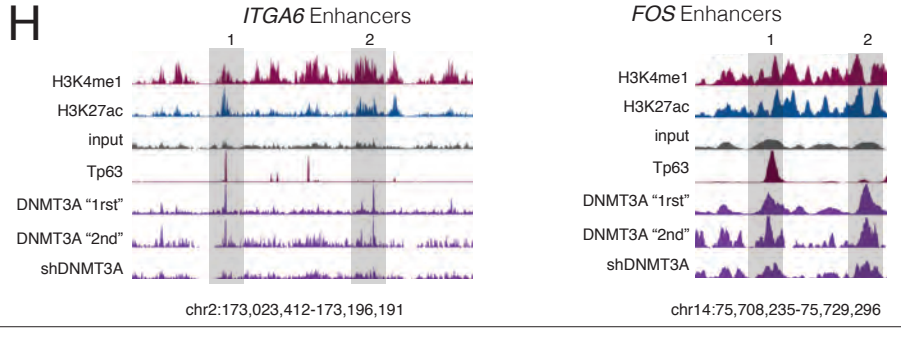

I

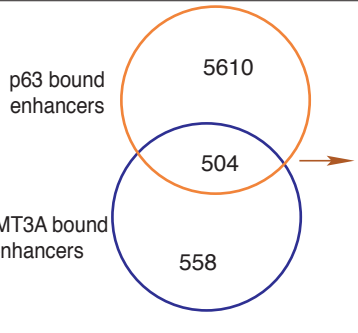

Common Regulated Enhancers

GO Terms	P-value
EGF Receptor Pathway	2.02e-06
Keratinocyte identity	6.08e-05
epithelial cell proliferation	3.68e-04
epidermis morphogenesis	3.43e-03

J

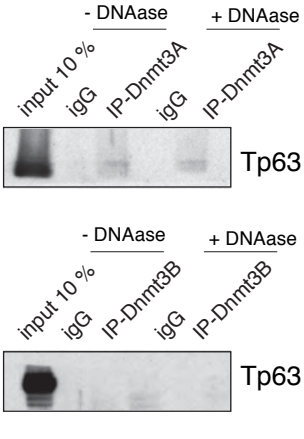

K

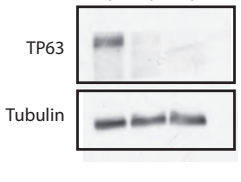

L

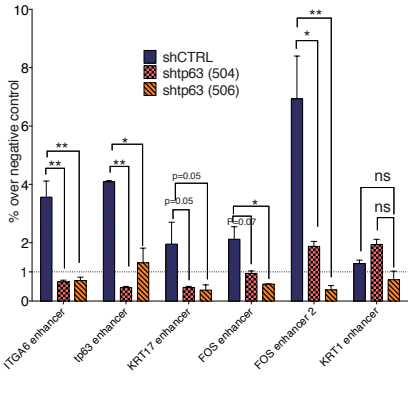

Figure

Figure 3

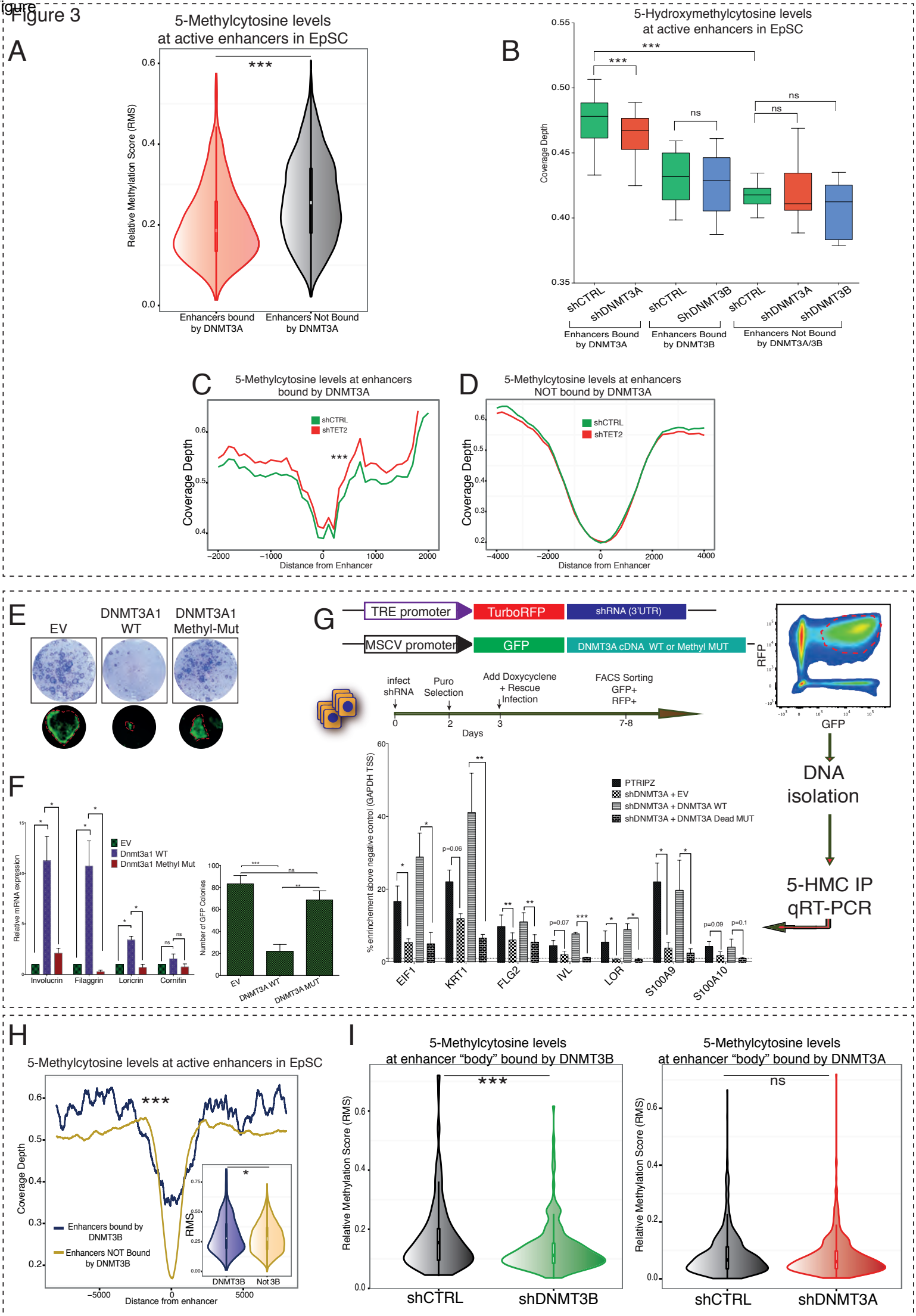

Figure Figure 4

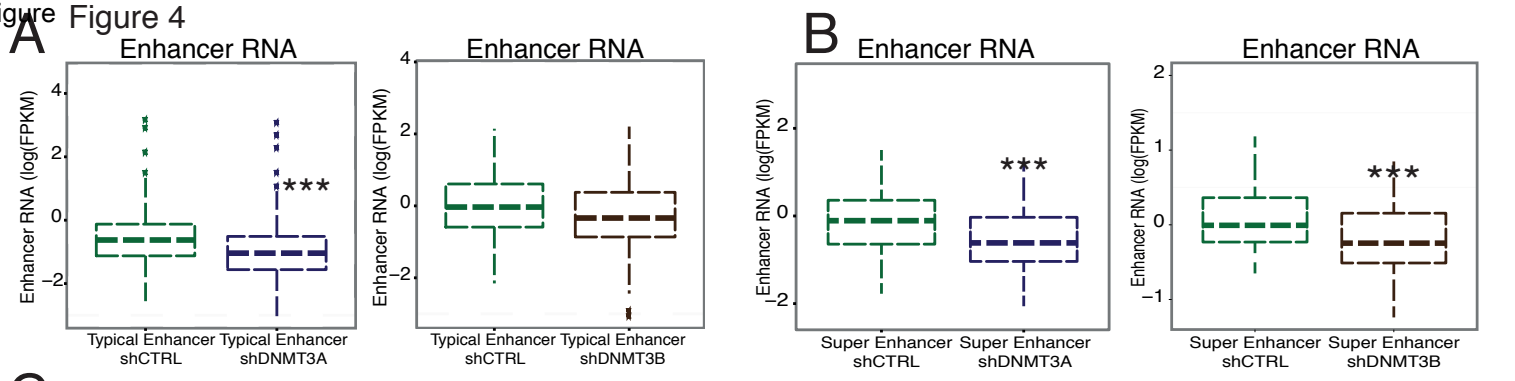

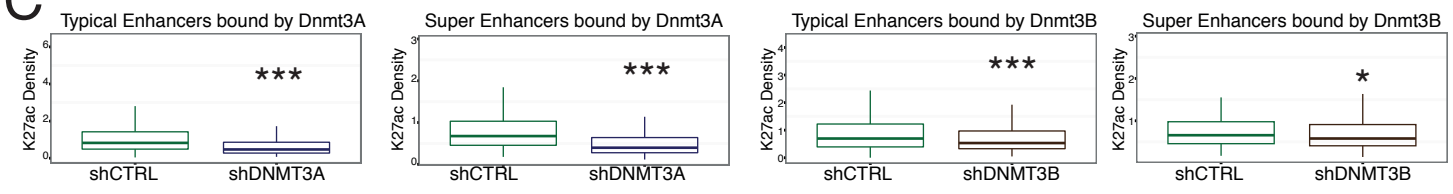

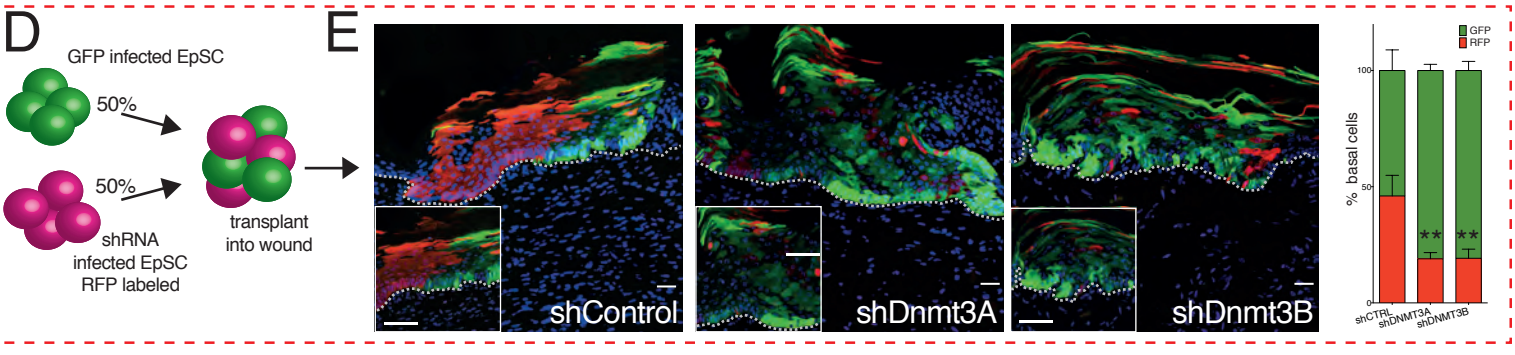

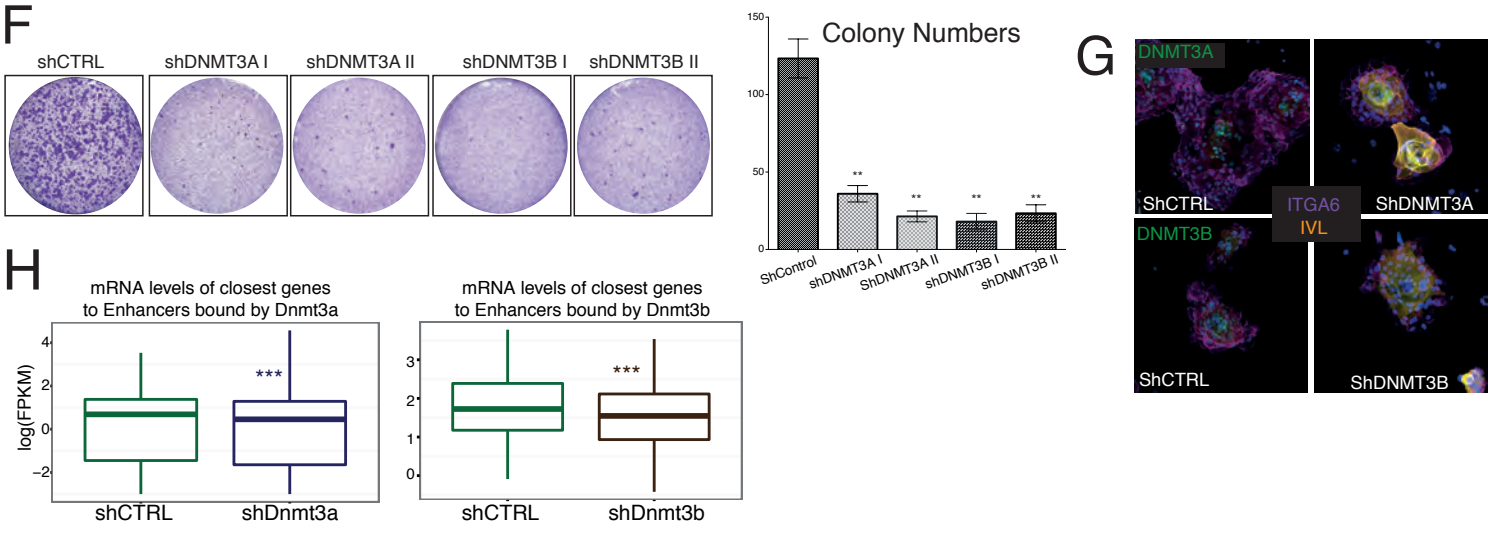

I

Downregulated in shDnmt3a

GO Terms	P-value
DNA repair	9.10E-13
DNA replication	1.81E-10
cell cycle	2.63E-07
TP53 pathway	6.06E-03

Upregulated in shDnmt3a

GO Terms	P-value
keratinocyte differentiation	2.92E-20
cell death	6.40E-15
RAS oncogenic pathway	8.57E-06
MAPK pathway	2.25E-06

Downregulated in shDnmt3b

GO Terms	P-value
mitosis	6.20E-12
CYCLIN B1 pathway	1.93E-05
cellular response to UV	1.43E-05
checkpoint	8.52E-03

Upregulated in shDnmt3b

GO Terms	P-value
epidermal cell differentiation	1.19E-13
NFKB pathway	5.13E-05
regulation of GTPase activity	3.51E-04
cell migration	4.66E-04

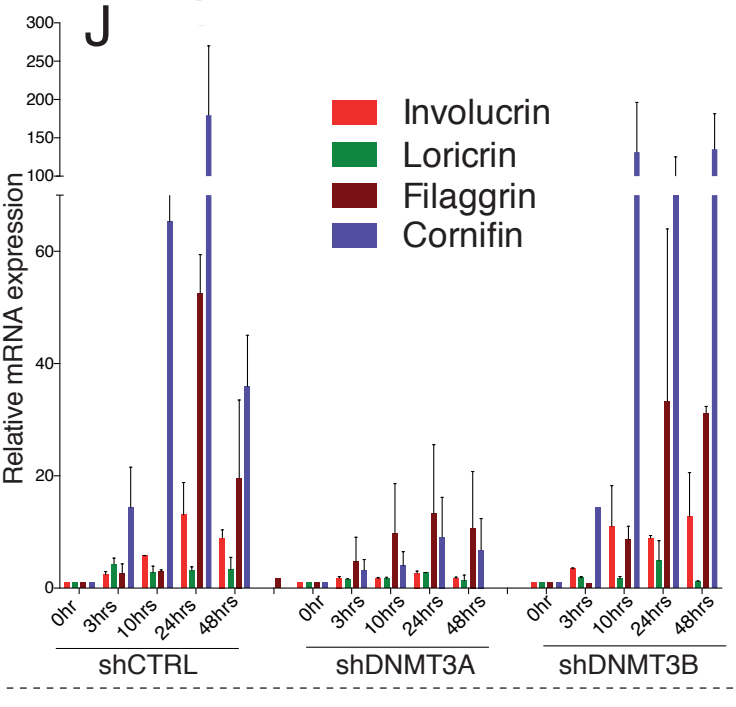

Supplemental Figures & Text

Figure S1

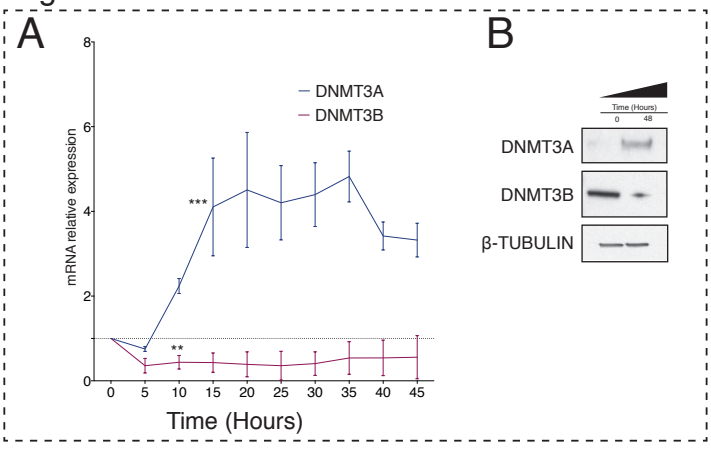

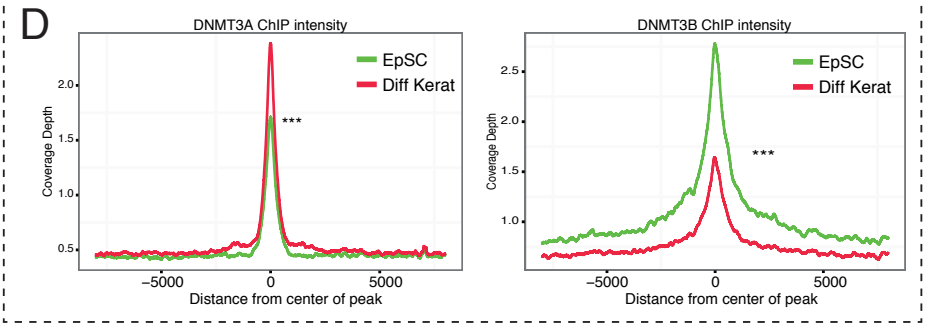

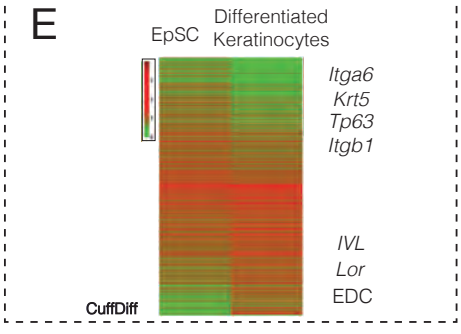

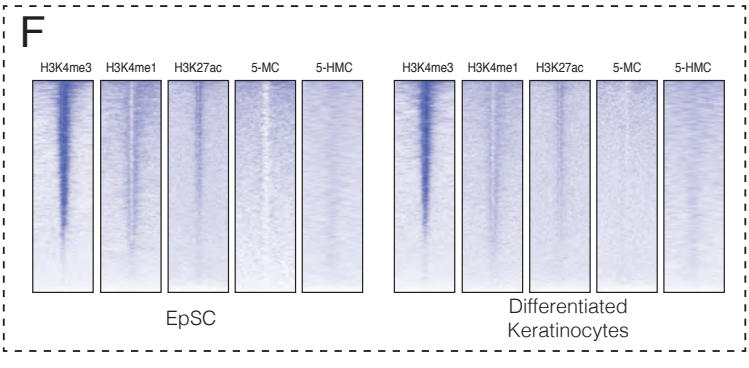

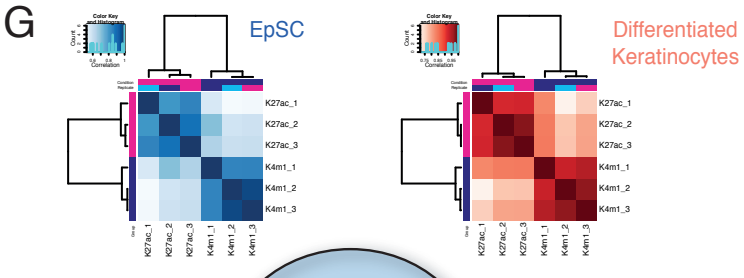

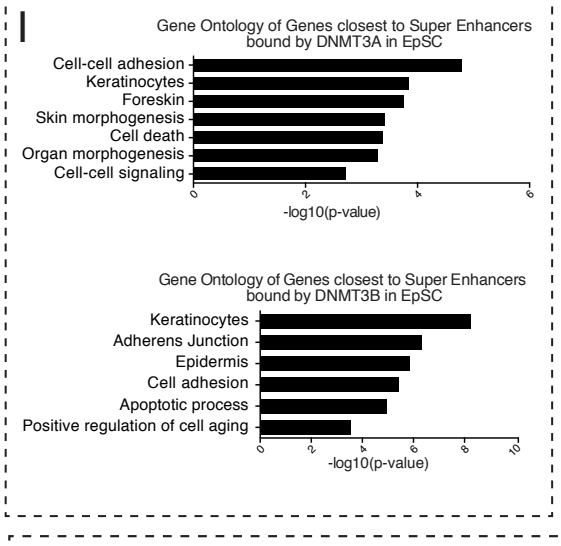

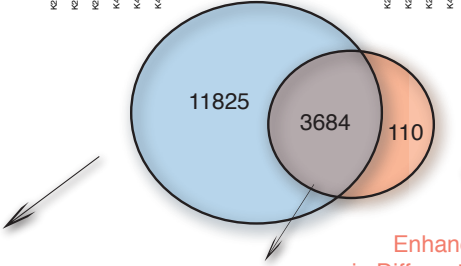

H

Enhancers active only in EpSC

GO Terms	P-value
cell cycle	1.66E-25
keratinocyte identity	5.79E-20
epidermis	1.12E-07
cell migration	1.10E-03

Enhancers active in both

GO Terms	P-value
keratinocyte identity	9.15E-11
signal transduction	8.54E-10
cell communication	9.82E-09
egulation of MAPK cascade	4.36E-04

Enhancers active only in Differentiated Keratinocytes

GO Terms	P-value
keratinocyte differentiation	1.04E-03
regulation cell polarity	2.12E-03
epidermal cell differentiation	3.80E-03
positive regulation GTP activity	8.70E-03

J

Enhancers bound by Dnmt3A in EpSC

Examples: *ITGA6, Tp63, FOS,KLF6*

GO Terms	P-value
cell proliferation	3.85E-07
keratinocyte identity	1.23E-07
epithelial cell migration	2.33E-07
epidermis development	9.37E-03

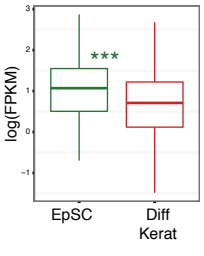

Enhancers bound by Dnmt3A in Diff Keratinocytes

Examples: *CRNN, KRT1, SCEL, TET2*

GO Terms	P-value
squamous epithelial cells	1.22E-04
cell differentiation	6.41E-04
epithelial cell differentiation	7.10E-04
epithelial cell migration	2.33E-03

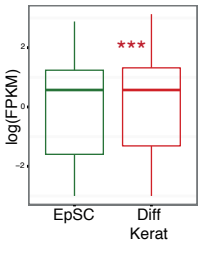

Figure S2

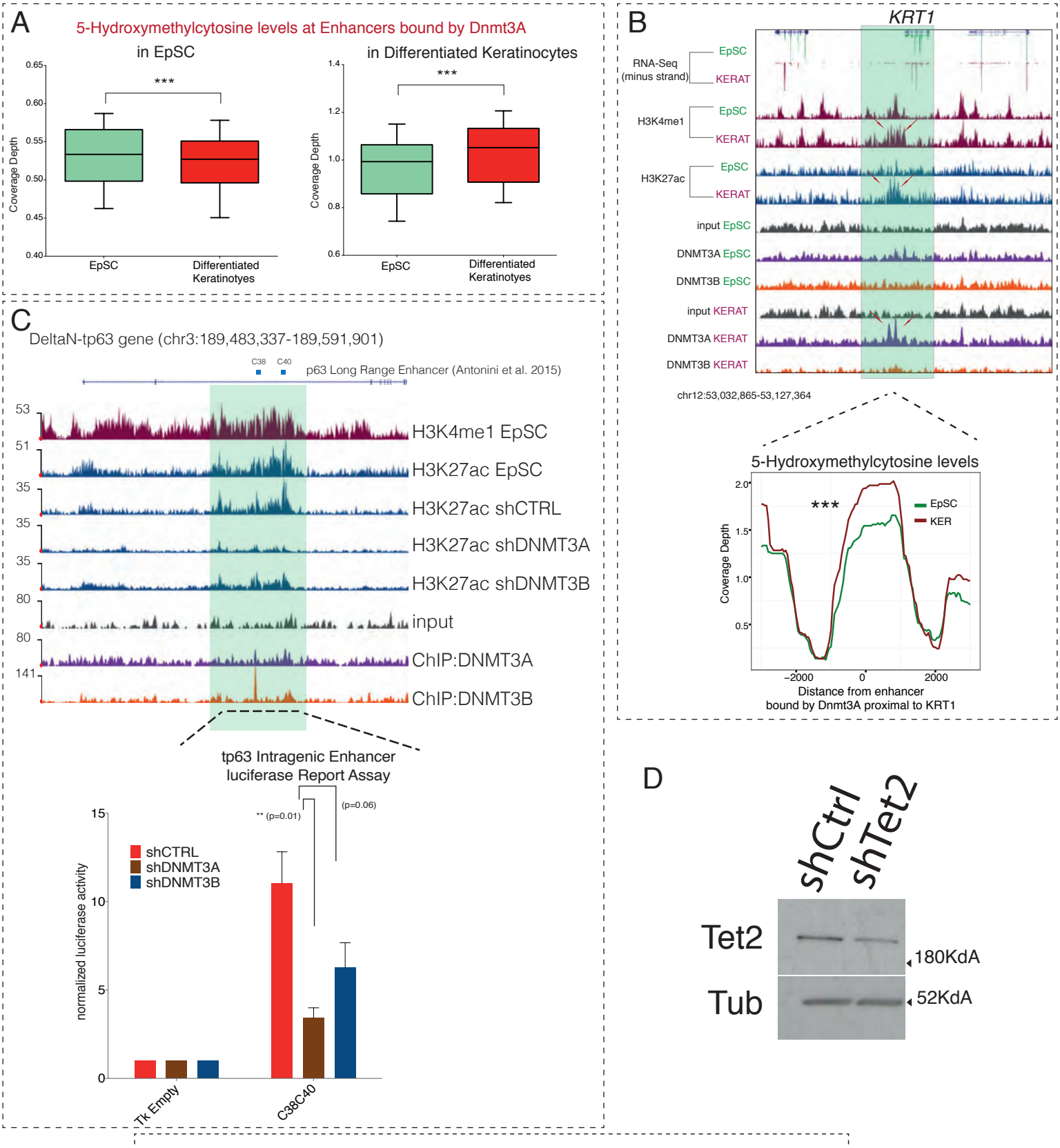
A
5-Hydroxymethylcytosine levels at Enhancers bound by Dnmt3A
in EpSC
in Differentiated Keratinocytes
***
Coverage Depth
EpSC
Differentiated Keratinotyes
B
KRT1
RNA-Seq (minus strand)
H3K4me1
H3K27ac
EpSC
KERAT
input EpSC
DNMT3A EpSC
DNMT3B EpSC
input KERAT
DNMT3A KERAT
DNMT3B KERAT
chr12:53,032,865-53,127,364
5-Hydroxymethylcytosine levels
KER
Distance from enhancer
bound by Dnmt3A proximal to KRT1
C
DeltaN-tp63 gene (chr3:189,483,337-189,591,901)
C38
C40
p63 Long Range Enhancer (Antonini et al. 2015)
H3K4me1 EpSC
H3K27ac EpSC
H3K27ac shCTRL
H3K27ac shDNMT3A
H3K27ac shDNMT3B
input
ChIP:DNMT3A
ChIP:DNMT3B
tp63 Intragenic Enhancer
luciferase Report Assay
** (p=0.01)
(p=0.06)
shCTRL
shDNMT3A
shDNMT3B
normalized luciferase activity
Tk Empty
C38C40
D
shCtrl
shTet2
Tet2
Tub
180KdA
52KdA
E
DNMT3A ChIP intensity
DNMT3B ChIP intensity
shCTRL
shDNMT3A
shDNMT3B
Distance from Enhancer
Bound by DNMT3A
Bound by DNMT3B

Figure S3

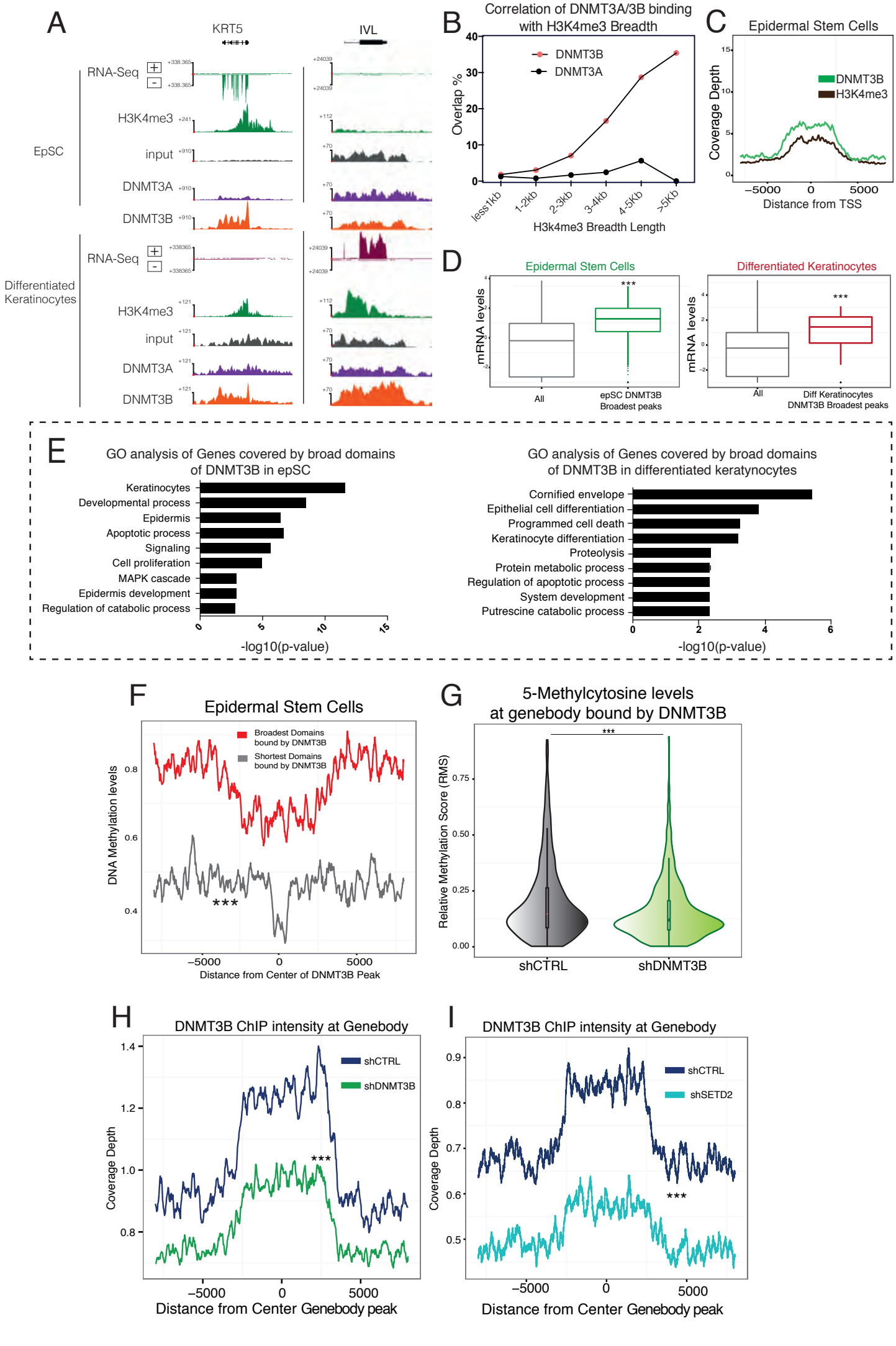
A
KRT5
IVL
RNA-Seq
H3K4me3
input
DNMT3A
DNMT3B
EpSC
Differentiated Keratinocytes
B
Correlation of DNMT3A/3B binding with H3K4me3 Breadth
DNMT3B
DNMT3A
Overlap %
less1kb
1-2kb
2-3kb
3-4kb
4-5Kb
>5Kb
H3k4me3 Breadth Length
C
Epidermal Stem Cells
DNMT3B
H3K4me3
Coverage Depth
Distance from TSS
D
Epidermal Stem Cells
Differentiated Keratinocytes
mRNA levels
All
epSC DNMT3B Broadest peaks
Diff Keratinocytes DNMT3B Broadest peaks
E
GO analysis of Genes covered by broad domains of DNMT3B in epSC
Keratinocytes
Developmental process
Epidermis
Apoptotic process
Signaling
Cell proliferation
MAPK cascade
Epidermis development
Regulation of catabolic process
-log10(p-value)
GO analysis of Genes covered by broad domains of DNMT3B in differentiated keratynocytes
Cornified envelope
Epithelial cell differentiation
Programmed cell death
Keratinocyte differentiation
Proteolysis
Protein metabolic process
Regulation of apoptotic process
System development
Putrescine catabolic process
-log10(p-value)
F
Epidermal Stem Cells
Broadest Domains bound by DNMT3B
Shortest Domains bound by DNMT3B
DNA Methylation levels
Distance from Center of DNMT3B Peak
G
5-Methylcytosine levels at genebody bound by DNMT3B
Relative Methylation Score (RMS)
shCTRL
shDNMT3B
H
DNMT3B ChIP intensity at Genebody
shCTRL
shDNMT3B
Coverage Depth
Distance from Center Genebody peak
I
DNMT3B ChIP intensity at Genebody
shCTRL
shSETD2
Coverage Depth
Distance from Center Genebody peak

Figure S4

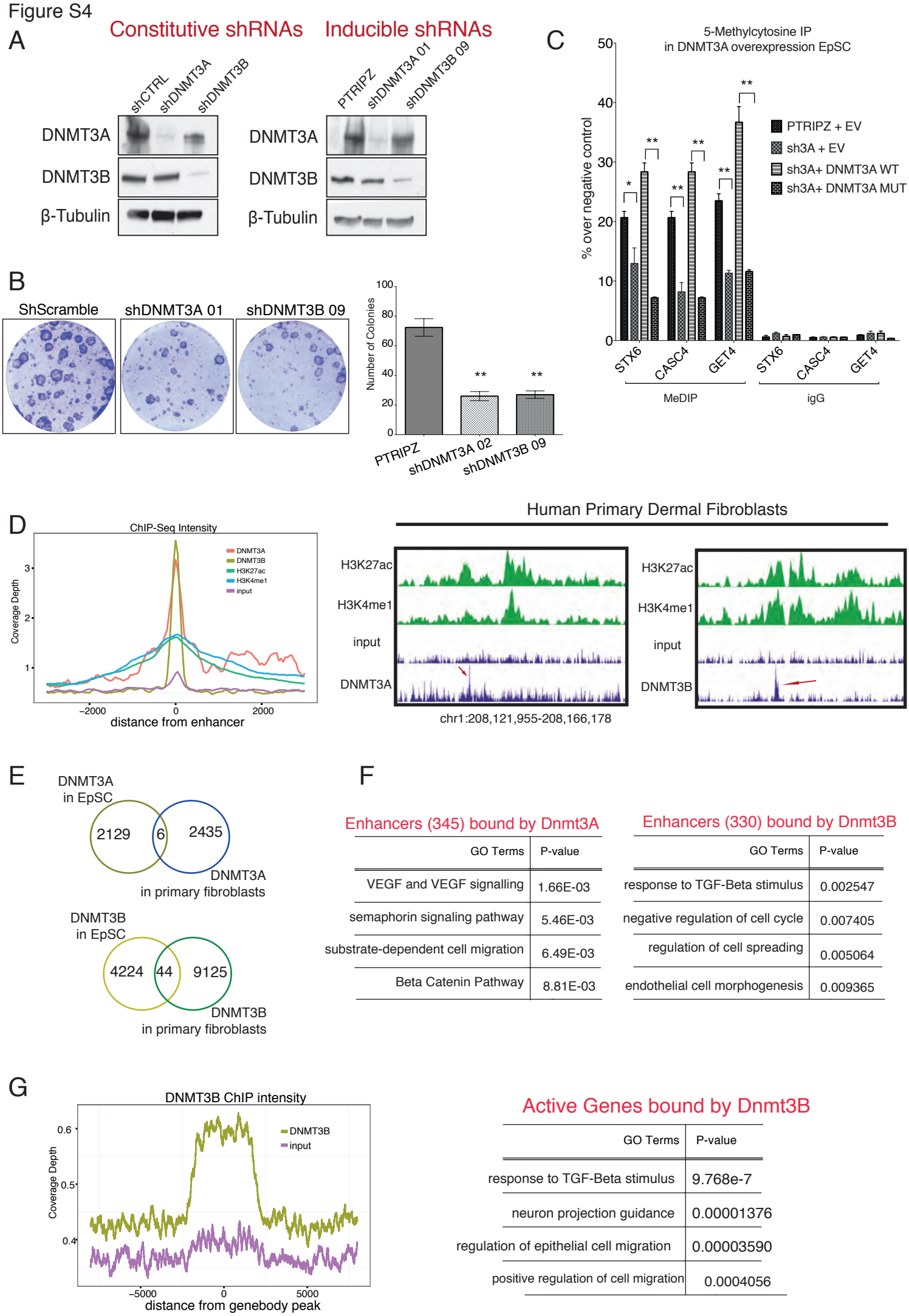

GO Terms	P-value
VEGF and VEGF signalling	1.66E-03
semaphorin signaling pathway	5.46E-03
substrate-dependent cell migration	6.49E-03
Beta Catenin Pathway	8.81E-03

GO Terms	P-value
response to TGF-Beta stimulus	0.002547
negative regulation of cell cycle	0.007405
regulation of cell spreading	0.005064
endothelial cell morphogenesis	0.009365

GO Terms	P-value
response to TGF-Beta stimulus	9.768e-7
neuron projection guidance	0.00001376
regulation of epithelial cell migration	0.00003590
positive regulation of cell migration	0.0004056

SUPPLEMENTARY INFORMATION

Figure S1 related to Figure 1. Dnmt3a and Dnmt3b Expression is Differentially Regulated During Human EpSC Differentiation mirroring dynamic behavior of enhancers between Human EpSC and differentiated keratinocytes. (A) RT-qPCR results confirming the differential expression of Dnmt3a and Dnmt3b during EpSC differentiation. RNA levels are normalized with respect to the PUM1 housekeeping gene (n = 5). (B) Western blot of EpSCs and differentiated keratinocytes for Dnmt3a, Dnmt3b. (C) Number of Dnmt3a or Dnmt3b peaks identified using Deseq2 in EpSCs and differentiated keratinocytes. (D) Dnmt3a and Dnmt3b ChIP-seq signal intensity at peaks defined as common using DeSeq2 in EpSCs and differentiated keratinocytes (E) Heatmap for RNA-seq (F) or ChIP-seq binding profiles for histone marks, Medip-Seq and 5-HydroxyMedip-Seq in EpSCs and differentiated keratinocytes. (G) Pearson correlation plot of ChIP-seq for H3K4me1 and H3K27ac replicates in EpSCs and in differentiated keratinocytes. (H) Upper panel, overview of active enhancer ($H3K4me1^{+}$ $H3K27ac^{+}$) dynamics during differentiation of EpSCs to differentiated keratinocytes. Differentially enriched enhancers were calculated with DeSeq2 using three biological replicates for each histone mark. Lower panel, gene ontology (GO) analysis (identified by proximity) of active enhancers in either EpSCs or differentiated keratinocytes or in both. (I) Gene ontology of the genes closest to super-enhancers bound by Dnmt3a/b in EpSCs. (J) Gene ontology and mRNA expression (small boxes) of the genes closest to the enhancers bound by Dnmt3a in EpSCs (left) or differentiated keratinocytes (right).

Figure S2 related to Figure 3. The Dynamic Binding of Dnmt3a at Enhancers Correlates with High Levels of 5-hmC. (A) Boxplots depicting hMeDIP-seq coverage depth (per bp per peak per 10 million mapped reads) at the intergenic enhancers bound by Dnmt3a only in EpSCs (left) or differentiated keratinocytes (right) (both with $p < 0.0001$). (B) Upper panel, UCSC genome browser screenshot of two enhancers bound in differentiated keratinocytes by Dnmt3a. All tracks show normalized and scaled raw sequencing reads. Lower panel, hMeDIP-seq coverage depth (per bp per peak per 10 million mapped reads) at the intergenic enhancers proximal to *KRT1* (right, $p = 5.62 \times 10^{-5}$). (C) Intragenic ΔNp63 enhancers bound by Dnmt3a and Dnmt3b, recently shown to drive ΔNp63 expression in embryonic and adult murine basal epidermal keratinocytes. Lower panel: C38C40-Luc enhancer activity were analyzed in shCTRL and Dnmt3a or Dnmt3b knockdown human stem cells after 48 hr of plasmid transfection. Data are expressed relative to the TK promoter activity used as control ($*p \leq 0.05$; $n = 3$). (D) Western blot for Tet2 protein and tubulin loading control in shCTRL and shTet2 in human EpSCs. (E) Enhancer binding was confirmed in two biological replicates. ChIP-seq coverage depth (per bp per peak per 10 million mapped reads) of Dnmt3a and Dnmt3b in shCTRL or Dnmt3a/b knockdown EpSCs.

Figure S3 related to Figure 3. Dnmt3b Spans Large Domains at the Gene Body of Highly Expressed Genes in an H3K36me3-dependent Manner. (A) UCSC screenshots of RNA-seq, H3K4me3, and ChIP-seq (using Dnmt3a, Dnmt3b, or input) of examples of gene body binding by Dnmt3b in stem cells and differentiated keratinocytes. (B) Percentage of genomic overlap between Dnmt3a/b binding sites

with H3K4me3 peak breadth. (C) Localization of H3K4me3 and Dnmt3b ChIP-seq signal in EpSCs, at the genes covered by the broadest domains of Dnmt3b. (D) RNA-seq expression values (log(FPKM)), both in EpSCs and in differentiated keratinocytes, of the genes bound by the broadest domains of Dnmt3b as compared to the all genes. Panel D, left side, $p < 2.2 \times 10^{-16}$; right side, $p = 1.579 \times 10^{-6}$. (E) Gene ontology analysis of genes covered by the broadest domains of Dnmt3b in EpSCs or in differentiated keratinocytes. (F) 5-methylcytosine levels at genes marked by the broadest and shortest domains of Dnmt3b. $p < 2.2 \times 10^{-16}$. (G) Relative methylation score measured at gene bodies bound by Dnmt3b in EpSCs infected with shCTRL vector or shDnmt3b vector ($p < 0.001$). (H) Depletion of Dnmt3b in EpSCs confirms the specificity of Dnmt3b binding to the gene bodies, as determined by ChIP-seq in shCTRL- and Dnmt3b-knockdown cells. (I) ChIP-seq coverage depth (per bp per peak per 10 million mapped reads) of Dnmt3b in shCTRL and SETD2 knockdown cells.

Figure S4 related to Figure 3. (A) Western blot of Dnmt3a and Dnmt3b proteins in control cells or cells infected with constitutive (left) or inducible (right) shRNA constructs targeting the expression of Dnmt3a or Dnmt3b. (B) Representative images of the clonogenic assay and quantification of colonies formed by human EpSCs infected with doxycycline-inducible shRNA vectors expressing shRNAs against Dnmt3a or Dnmt3b. (C) MeDIP-qPCR using 100,000 sorted RFP+GFP+ cells, expressing the shRNAs against endogenous Dnmt3a and the cDNA to ectopically express wild-type Dnmt3a1, or the methyltransferase mutant version (PC➔VD). Enrichment at the promoter region of the *STX6, CASC4*, and *GET4* genes was calculated by normalizing the value of the GAPDH TSS, a region negative for DNA

methylation. (D) Left panel: ChIP-seq coverage depth (per bp per peak per 10 million mapped reads) of input, H3K4me1, H3K27ac, Dnmt3a, or Dnmt3b in human primary dermal fibroblasts. Right panel: UCSC genome browser screenshot of examples of Dnmt3a/b binding at active enhancers in human primary dermal fibroblasts. (E) Number of peaks overlapping between ChIP-seq of Dnmt3a and Dnmt3b in EpSCs and in primary human dermal fibroblasts. (F) Gene ontology of genes closest to enhancers (H3K4me1 and H3K27ac ChIP-seq from dermal fibroblasts obtained from the ENCODE database) bound by Dnmt3a or Dnmt3b. (G) Left panel, ChIP-seq coverage depth (per bp per peak per 10 million mapped reads) of input and Dnmt3b in active gene bodies in primary human dermal fibroblasts. Right panel, gene ontology of genes bound by Dnmt3b at gene bodies.

SUPPLEMENTARY TABLES

Table S1 related to Figure S1 and Figure 1. It contains the fpkm values of genes and all specific isoforms expressed in epidermal stem cells and differentiated keratinocytes.

Table S2 related to Figure S1 and Figure 1. Sheet A, contains the genomic coordinates of the ChIP-seq peaks of Dnmt3a and Dnmt3b in stem cells and differentiated keratinocytes used in the manuscript to describe the regulation of Dnmt3a and Dnmt3b in EpSC homeostasis. Sheet B contains the Pearson Correlation coefficient of the two biological replicates of Dnmt3a and Dnmt3b Chip-seq.

Table S3 related to Figure S1, Figure S3, Figure 1, Figure 2 and Figure 3. Sheet A contains the genomic coordinates of the ChIP-seq peaks of H3K4me1, H3K4me3 and H3K27ac in stem cells and differentiated keratinocytes. Sheet B contains the consensus enhancers found in EpSC and in Differentiated Keratinocytes using three biological replicates and used for DeSeq2 differential enrichment analysis. Sheet C shows the list of genes closest to active enhancers in epidermal stem cells, and enhancers that become *de novo* active or remain active upon keratinocyte differentiation, using standard MACS2 peak calling.

Table S4 related to Figure 4. Sheet A contains data classifying enhancers into typical and super-enhancers in stem cells and for differentiated keratinocytes. It also contains the signal and read density data of Dnmt3a and Dnmt3b at the enhancers.

Sheet B contains enhancer RNA values in stem cells and differentiated keratinocytes, and in knockdown cells, respectively.

Sheet C, relates to Figure S3 and contains the lists of genes that are covered by broad domains of Dnmt3b in stem cells and differentiated keratinocytes.

Sheet D, relates to Figure4 and contains the lists of genes that are downregulated or upregulated in Dnmt3a and Dnmt3b knockdown cells.

SUPPLEMENTARY METHODS

Human EpSC Culture and Calcium-induced Differentiation

Human EpSCs were isolated independently from three neonatal foreskin samples and cultured with a feeder layer of fibroblasts (J2-3T3) as described previously (Janich et al., 2013). Undifferentiated keratinocytes were grown in keratinocyte serum-free medium (KSFM) with supplements as indicated by the manufacturer (GIBCO). For calcium-induced differentiation, KSFM was exchanged for EMEM (Lonza) supplemented with 8% chelated FBS, EGF (10 ng/ml), 1% penicillin/streptomycin, and 1.2 mM $CaCl_2$, once cells had reached 70% confluence. After 48 hr, differentiated keratinocytes were collected for analysis.

Lentiviral Infections

EpSCs growing in KSFM media were infected with precipitated lentiviral particles produced by 293T cells and transfected with the above-mentioned plasmids, as previously described (Janich et al., 2013; Luis et al., 2011). Cells were collected for RNA extraction or ChIP assay after 5 to 7 days of puromycin selection.

Chromatin immunoprecipitation–sequencing (ChIP-seq)

ChIP was performed as previously described (Morey et al., 2012). Briefly, EpSCs and differentiated keratinocytes were trypsinized and crosslinked in 1% formaldehyde for 10 min at room temperature. Crosslinking was quenched with 0.125 M glycine. Pelleted cells were lysed in 1 ml ChIP buffer (2:1 solution of 100 mM NaCl, 50 mM Tris-HCl, 5 mM EDTA, 0.5% SDS, 100 mM NaCl, 5 mM EDTA, and 5% Triton X-100) and sonicated for 15 min in a Bioruptor (Diagenode). Soluble material was

quantified by Bradford assays. To immunoprecipitate transcription factors, 2 mg of protein and 100 μg of immunoprecipitated histone/histone modifications were used. Antibodies (10 μg for Dnmt3a/3b and 3 μg for histone modifications) were incubated overnight with the chromatin in ChIP buffer. Immunocomplexes were recovered with 30 μl of protein A bead slurry (Healthcare, 17-5280-01). Immunoprecipitated material was washed three times with low salt buffer (50 mM HEPES pH 7.5, 140 mM NaCl, 1% Triton) and 1× with high salt buffer (50 mM HEPES pH 7.5, 500 mM NaCl, 1% Triton). DNA complexes were de-crosslinked at 65°C overnight, and DNA was then eluted in 50 μl of water using the PCR purification kit (QIAGEN). Antibodies used for ChIP or MedIP were Dnmt3a (SantaCruz H-295), Dnmt3b (Novus Biotechnology, NB100-266), H3K27ac (Merck Millipore, 07-360), H3K4me1 (Abcam, ab8895), and H3K4me3 (Diagenode, C15410003-50), and H3K36me3 (Abcam, ab9050). Libraries for sequencing were prepared using NEBNext Ultra DNA Library Prep Kit for Illumina (E7370L) following the manufacturer's instructions.

MeDIP and hMeDIP sequencing

Purified genomic DNA (500 ng) from cells was sonicated to obtain fragments of 300–700 bp. Adaptors from the NEBNext Ultra DNA Library Prep Kit for Illumina were added to the fragmented DNA. DNA was denatured for 10 min at 99°C and cooled down to avoid re-annealing. Fragmented DNA was incubated 2 hr with 1 μg of 5-methylcytosine (Eurogentec, BI-MECY-0100) or 5-hydroxymethylcytosine (Active Motif, 39769). Immunocomplexes were recovered using 8 μl of Dynabeads Protein A (Life Technologies) for 2 hr. Purified DNA was extracted using QIAquick MinElute (Qiagen). Amplified libraries were prepared using NEBNext Ultra DNA Library Prep Kit for Illumina (E7370L) following manufacturer's instructions.

ChIP-seq Data Processing

The ChIP-seq datasets were aligned to the Human Genome hg19 using Bowtie (version 1.0.1) (Langmead et al., 2009), using the parameters –k 1, –m 1, and –n 2. Peak calling of Dnmt3a and Dnmt3b to determine regions of ChIP-seq enrichment over the background was done with the MACS version 1.4.1., using parameters –p 1e–5, –w, –S, and –g hs[5]. Peaks of the methylation and hydroxymethylation datasets were determined similarly, but with the parameter p set to 1e–3. For histone marks, the MACS version 2 was used with parameters –broad, -q 0.01, and –g hs. UCSC browser tracks (Kent et al., 2002) were created from the MACS wiggle or bedgraph output. ChIP-seq peaks were annotated using the annotatePeaks.pl script of the HOMER suite (version 4.6) (Heinz et al., 2010) using the UCSC hg19 annotation. The coverage depths of different ChIP-seq experiments at specified regions were also calculated using the annotatePeaks.pl script. This generates a normalized coverage value of different sequencing experiments at equally-spaced bins spanning the region of interest. The bin size was set to 25 bp.

For the differential regulation analysis of ChIP-seq data with replicates, the R package DiffBind (http://bioconductor.org/packages/release/bioc/vignettes/DiffBind/inst/doc/DiffBind.pdf) was used, with DESeq2 (Love et al., 2014) applied to calculate the differentially bound regions using padj < 0.1. The differential regions were called on a set of consensus peaks (e.g., peaks present in at least 2 out of 3 replicates for cases with 3 replicates, and merging peaks for cases with 2 replicates).

RNA Library Preparation and Sequencing

The library from total RNA from three biological replicates was prepared using the TruSeq®Stranded Total Sample Preparation kit (Illumina Inc.) according to the manufacturer's protocol. Briefly, rRNA was depleted from 0.5 μg of total RNA using the Ribo-Zero Gold Kit, followed by fragmentation by divalent cations at elevated temperature, resulting into fragments of 80–450 nt, with the major peak at 160 nt. First-strand cDNA synthesis by random hexamers and reverse transcriptase was followed by the second-strand cDNA synthesis, performed in the presence of dUTP instead of dTTP. Blunt-ended double-stranded cDNA was 3′-adenylated, and the 3′-"T" nucleotide at the Illumina indexed adapters was used for the adapter ligation. The ligation product was amplified with 15 cycles of PCR. Each library was sequenced using TruSeq SBS Kit v3-HS, in paired end-mode with the read length 2 × 76 bp. A minimal of 137 million paired-end reads were generated for each sample run in one sequencing lane on HiSeq2000 (Illumina, Inc) following the manufacturer's protocol. Images analysis, base calling, and quality scoring of the run were processed using the manufacturer's software Real-Time Analysis (RTA 1.13.48) and followed by generation of FASTQ sequence files by CASAVA.

RNA-seq Data Processing

RNA-seq datasets were aligned to the Human Genome hg19 using the GEM split mapper version 7.0 (Marco-Sola et al., 2012) with default parameters. To quantify the gene and transcript expression levels, Cufflinks (version 2.1.1) (Trapnell et al., 2010) was run with UCSC hg19 reference annotations, providing FPKM (fragments per kilobase of exon per million fragments mapped) values. Differentially expressed genes were obtained using Cuffdiff from the Cufflinks suite. A q-value cutoff of 0.001 was used for identifying differentially expressed genes.

Enhancer Analysis

Enhancers were divided into two classes: poised and active. Poised enhancers were defined as regions with peaks of H3K4m1 but not of H3K27ac, while active enhancers were defined as regions with peaks of both H3K4m1 and H3K27ac. Enhancer regions were annotated using the HOMER suite. Enhancer RNA FPKM values were calculated by obtaining the number of RNA-seq reads falling within the enhancer region and normalizing it by the enhancer length and number of mapped reads. To generate the enhancer RNA box plots, only intergenic enhancer regions were considered.

Super-enhancer Analysis

Super-enhancers (SEs) were detected using the ROSE software (https://bitbucket.org/young_computation/rose). The software was run with default parameters, with peaks of H3K27ac considered as constituent enhancers. Briefly, ROSE stitches together enhancer regions within 12.5 kb (default) of one another. The stitched enhancer regions were ranked by the H3K27ac signal present in them. From the graph of H3K27ac signal versus enhancer rank, the enhancers residing above the inflexion point of the curve were designated as SEs, while the rest were designated as normal enhancers. ROSE outputs the H3K27ac read density in units of reads-per-million mapped per bp (rpm/bp) of each stitched enhancer. SE and typical enhancer regions were considered to contain Dnmt3A and Dnmt3B if there was an overlap with Dnmt3A and Dnmt3B peaks, respectively. To quantify the signal strength of Dnmt3A and Dnmt3B in typical enhancers and SEs, the read densities of Dnmt3A, Dnmt3B, and the input were calculated in units of rpm/bp of each enhancer region. For further

consideration, the background-subtracted density for an enhancer region was required to be at least 0.05 rpm/bp. For both typical enhancers and SEs, the mean of the background subtracted ChIP-seq signal (total reads) and the mean of the signal density was calculated. The fold differences shown in Figure 3 refer to the ratios of these means between SEs and typical enhancers.

Relative Methylation Score

Relative methylation score (RMS) was calculated using the MEDIPS (1) package. MEDIPS calculates normalized methylation levels (RMS) by building a linear model which represents the dependency of CpG densities and the MeDIP-seq counts across the entire range of CpG densities (Lienhard et al., 2014). RMS values were calculated using MEDIPS at 100 bp windows across the genome. These values were used to calculate the RMS values at enhancers and gene bodies bound by Dnmt3b. The function used for this purpose was MEDIPS.selectROIs with the "summarize=avg" option; thus the RMS values in the windows inside the enhancers and gene bodies are averaged.

Enhancer "body" is defined as the region flanking the enhancer center. It was calculated on average for SEs and typical enhancers to be between –/+4 KB from the enhancer center. The RMS value of the enhancer body was calculated using unique aligned reads at a distance of –/+4KB from the center of enhancer, found by the intersection of H3K4me1 and H3K27ac peaks in intergenic regions.

Statistical Significance Tests

For all boxplots, p values for statistical significance were calculated using a Wilcoxon signed-rank test. A two-sample Kolmogorov-Smirmov test was used to calculate the statistical significance between coverage density plots.

Immunofluorescence

Human EpSCs grown on glass coverslips were fixed in 4% paraformaldehyde for 10 min, permeabilized with 0.5 % Triton/ PBS for 10 min, blocked with 0.25% BSA/PBS for 45 min, and stained with primary and secondary antibodies diluted in blocking buffer for 60 min at room temperature. Nuclei were counterstained with DAPI (Roche). Primary antibodies were anti-involucrin (1:1,000; Abcam, ab68), anti-DNMT3A (1:100, SantaCruz), and DNMT3B (1:200, Novus Biotech); secondary antibodies were anti-rabbit Alexa Fluor 647 and anti-mouse Alexa Fluor 594 (1:500, Molecular Probes). Pictures were acquired using a Leica TCS SP5 confocal microscope. Protein extracts were analyzed by SDS-PAGE, and western blotting for DNMT3a (1:500 SantaCruz) and DNMT3b (1:1000 Novus Biol).

RT-qPCR

RNA was extracted using TRIzol (SIGMA®) and converted into cDNA by reverse transcriptase using the TaqMan Applied Biosystem® kit. Gene expression was quantified by quantitative real-time PCR using SYBR Green (Applied Biosystem) master mix.

Mutagenesis of Dnmt3a1 and Dnmt3b1 Wild-type Isoforms

Dnmt3a1 and Dnmt3b1 cDNA isoforms were ordered from Addgene and cloned into the pMSCV PIG (Puro-Ires-GFP) retroviral backbone vector. Point mutations were

inserted using the Agilent Quikchange II XL Mutation Kit using the following primers:

Dnmt3a1, methyl mutation, from PC➔VD, using the primers:

FW 5′-TTGGGGGCAGTGTCGACAATGACCTCTCC-3′

RV 5′-GGAGAGGTCATTGTCGACACTGCCCCCAA-3′

Dnmt3a1, PWWP mutation, from WP➔ST, using the primers:

FW 5′-CAATGCGGCCCGTCGACCAGGAGAAGCCCCGCA-3′

RV 5′-TGCGGGGCTTCTCCTGGTCGACGGGCCGCATTG-3′

Dnmt3b1, methyl mutation, from PC➔GT, using the primers:

FW 5′-TTGGCGGAAGCGGTACCAACGATCTCTC-3′

RV 5′-GAGAGATCGTTGGTACCGCTTCCGCCAA-3′

Dnmt3b1, PWWP point mutation, from WP➔ST, using the primers:

FW 5′-CCATGGCGGTCGACCAGGAGAAGCCCTTG-3′

RV 5′-CAAGGGCTTCTCCTGGTCGACCGCCATGG-3′

Inducible shRNAs

TRIPZ doxycycline inducible vectors were purchased from Dharmacon. TRIPZ shRNA was used as a scramble control. shDnmt3b 02 (V3THS_402302) was selected as the best shRNA purchased from Dharmacon and was used directly as an shRNA against the 3′UTR of Dnmt3b. To obtain a Dnmt3a 3′UTR shRNA, the following sequence was inserted into the TRIPZ vector using EcoRI and XhoI for cutting and pasting.

5′TGCTGTTGACAGTGAGCGAGCATCCACTGTGAATGATAAGTAGTGAAGC
CACAGATGTACTTATCATTCACAGTGGATGCCTGCCTACTGCCTCGGA3′

Mutation Infections

Primary human keratinocytes grown in KSFM medium were infected for two consecutives days overnight with doxycycline-inducible shRNAs against DNMT3A or DNMT3B 3′UTR, or against a random sequence (TRIPZ). On the third day, doxycycline was added to the medium at a final concentration of 5 μg/ml, and cells were infected for three consecutive days (with a 4 to 5 hr incubation) with a retroviral vector expressing GFP and the cDNA of Dnmt3a1 or Dntm3b1 (wild-type or mutant isoforms). Double-positive RFP+ and GFP+ cells were maintained in doxycycline and puromycin for 2 extra days, trypsinized, and sorted by FACS using a FACS ARIA machine (BD Biosciences), prior to transplanting them into immunocompromised mice.

Western Immunoblotting

Proteins were extracted using RIPA buffer (4% SDS, 20% glycerol, 10% 2-mercaptoethanol, 0.004% bromophenol blue, and 0.125 Tris-HCl). Protein concentrations were quantified using BioRAD® BCA protein assay kit (Bio-Rad, 23227). Lysates were separated by a 10% SDS-PAGE gel, transferred to a nitrocellulose membrane, and incubated with rabbit anti-Dnmt3a (Santa Cruz 1:1000), rabbit anti-Dnmt3b (Novus 1:1000), and/or mouse anti-tubulin (Santa Cruz) (used as a loading control). TP63 antibody was purchased from Abcam (Ab53039) and used 1:1000 for western blot after endogenous immunoprecipitation of Dnmt3a or Dnmt3b.

Luciferase Reporter Assay

Primary human keratinocytes cultured in 12-well plates in KSFM medium were infected 2× for 4 hr with the short hairpin RNA constructs shCTRL, shDNMT3a, or shDNMT3b cloned in the pLKO lentiviral vector. After puromycin selection, infected cells at 80% confluence were transfected with 500 μl KSFM medium that had been pre-incubated with 3 μl of lipofectamine (Thermo Fisher Scientific, 11668027) containing 1 μg of the TK-empty or the TK-C38/C40 (p63 enhancer) luciferase plasmids, and 100 ng of the Renilla luciferase control plasmid. Incubation medium was changed for fresh KSFM after 6 hrs. Luciferase intensity was measured using the Dual-Luciferase Reporter Assay (Promega, e1910) according to the manufacturer's protocol.

Gene ontology

Gene ontology (GO) analyses was done using Genomatix (https://www.genomatix.de/), using the Gene Ranker package, with a p value of 0.01 and an adjusted p value of 0.05.

Skin Reconstitution Assay

For each transplant, 3×10^6 primary human keratinocytes infected with the TRIPZ vector expressing RFP and shCtrl, shDntm3a, or shDnmt3b were first mixed with 3 million keratinocytes infected with a GFP-expressing vector, then mixed with 4×10^6 newborn (P2) mouse fibroblasts, and transplanted onto the back of Swiss Nude mice as previously described (Lichti et al., 2008). shRNA expression was induced by administering 2 mg/ml of doxycycline in 5% sucrose drinking water. Skin grafts were

collected 4 weeks after transplantation, fixed for 2 hr in 4% PFA, and embedded in OCT for cryosections. Nuclei were stained with DAPI (1:10000). Pictures of direct fluorescence were acquired using a Leica SP5 confocal microscope.

Clonogenic Assay

Clonogenic assays were performed as previously described (Janich et al., 2013). Briefly, EpSCs growing on feeders were infected with precipitated lentiviral particles produced by 293T cells transfected with the mentioned plasmids. Puromycin-resistant primary keratinocytes were selected and detached from the feeder layer, and 1000 keratinocytes were seeded again on a new layer of feeder fibroblasts. These were cultured for at least 14 days, after which they were fixed for 20 min with 10% formalin, washed 2× with PBS, and stained with a mixture of Rhodamil Blue (0.5%) and Crystal Violet (0.5%) for 30 min.

Supplementary references

Heinz, S., Benner, C., Spann, N., Bertolino, E., Lin, Y.C., Laslo, P., Cheng, J.X., Murre, C., Singh, H., and Glass, C.K. (2010). Simple combinations of lineage-determining transcription factors prime cis-regulatory elements required for macrophage and B cell identities. Mol Cell *38*, 576–589.

Janich, P., Toufighi, K., Solanas, G., Luis, N.M., Minkwitz, S., Serrano, L., Lehner, B., and Benitah, S.A. (2013). Human EpSC function is regulated by circadian oscillations. Cell Stem Cell *13*, 745–753.

Kent, W.J., Sugnet, C.W., Furey, T.S., Roskin, K.M., Pringle, T.H., Zahler, A.M., and Haussler, D. (2002). The human genome browser at UCSC. Genome Res *12*, 996–1006.

Langmead, B., Trapnell, C., Pop, M., and Salzberg, S.L. (2009). Ultrafast and memory-efficient alignment of short DNA sequences to the human genome. Genome Biol *10*, R25.

Lichti, U., Anders, J., and Yuspa, S.H. (2008). Isolation and short-term culture of

primary keratinocytes, hair follicle populations and dermal cells from newborn mice and keratinocytes from adult mice for in vitro analysis and for grafting to immunodeficient mice. Nat Protoc *3*, 799–810.

Lienhard, M., Grimm, C., Morkel, M., Herwig, R., and Chavez, L. (2014). MEDIPS: genome-wide differential coverage analysis of sequencing data derived from DNA enrichment experiments. Bioinformatics *30*, 284–286.

Love, M.I., Huber, W., and Anders, S. (2014). Moderated estimation of fold change and dispersion for RNA-seq data with DESeq2. Genome Biol *15*, 550.

Luis, N.M., Morey, L., Mejetta, S., Pascual, G., Janich, P., Kuebler, B., Cozutto, L., Roma, G., Nascimento, E., Frye, M., et al. (2011). Regulation of human EpSC proliferation and senescence requires polycomb- dependent and -independent functions of Cbx4. Cell Stem Cell *9*, 233–246.

Marco-Sola, S., Sammeth, M., Guigo, R., and Ribeca, P. (2012). The GEM mapper: fast, accurate and versatile alignment by filtration. Nat Methods *9*, 1185–1188.

Morey, L., Pascual, G., Cozzuto, L., Roma, G., Wutz, A., Benitah, S.A., and Di Croce, L. (2012). Nonoverlapping functions of the Polycomb group Cbx family of proteins in embryonic stem cells. Cell Stem Cell *10*, 47–62.

Trapnell, C., Williams, B.A., Pertea, G., Mortazavi, A., Kwan, G., van Baren, M.J., Salzberg, S.L., Wold, B.J., and Pachter, L. (2010). Transcript assembly and quantification by RNA-Seq reveals unannotated transcripts and isoform switching during cell differentiation. Nat Biotechnol *28*, 511–515.

Click here to access/download

Supplemental Movies & Spreadsheets

Table S1.xlsx

Click here to access/download

Supplemental Movies & Spreadsheets

Table S2.xlsx

Click here to access/download

Supplemental Movies & Spreadsheets

Table S3.xlsx

Click here to access/download

Supplemental Movies & Spreadsheets

Table S4.xlsb